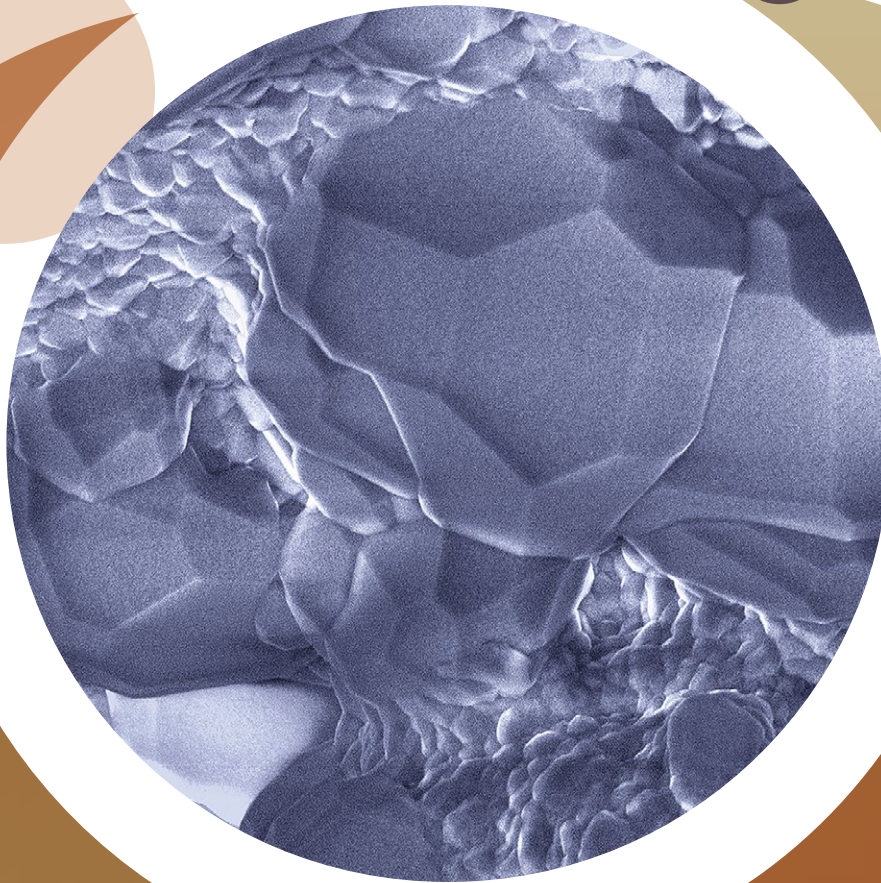


# Summary of the History and Research of the U.S. Geological Survey Gas Hydrate Properties Laboratory in Menlo Park, California, Active from 1993 to 2022

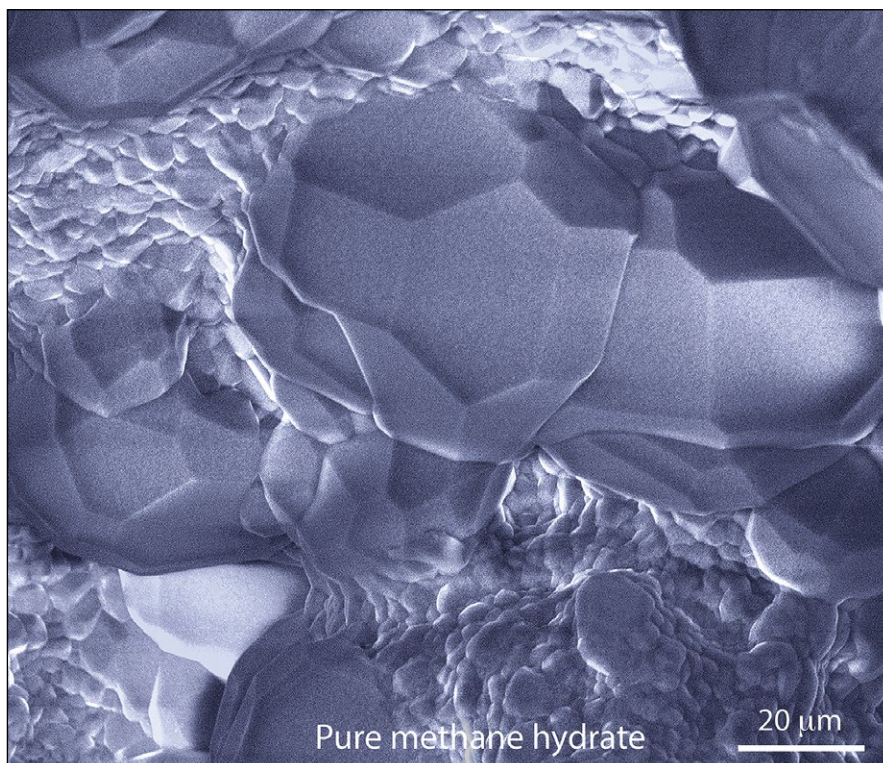


Open-File Report 2023–1063

**Cover.** Methane clathrate hydrate crystals in laboratory-made material formed by melting granulated ice in the presence of pressurized methane gas. Imaged by cryogenic scanning electron microscopy at  $-180$  degrees Celsius. Photo by L. Stern.

# Summary of the History and Research of the U.S. Geological Survey Gas Hydrate Properties Laboratory in Menlo Park, California, Active from 1993 to 2022

Laura A. Stern and Stephen H. Kirby



Open-File Report 2023–1063

**U.S. Department of the Interior**  
**U.S. Geological Survey**

## U.S. Geological Survey, Reston, Virginia: 2023

For more information on the USGS—the Federal source for science about the Earth, its natural and living resources, natural hazards, and the environment—visit <https://www.usgs.gov> or call 1–888–392–8545.

For an overview of USGS information products, including maps, imagery, and publications, visit <https://store.usgs.gov/> or contact the store at 1–888–275–8747.

Any use of trade, firm, or product names is for descriptive purposes only and does not imply endorsement by the U.S. Government.

Although this information product, for the most part, is in the public domain, it also may contain copyrighted materials as noted in the text. Permission to reproduce copyrighted items must be secured from the copyright owner.

Suggested citation:

Stern, L.A., and Kirby, S.H., 2023, Summary of the history and research of the U.S. Geological Survey gas hydrate properties laboratory in Menlo Park, California, active from 1993 to 2022: U.S. Geological Survey Open-File Report 2023–1063, 29 p., <https://doi.org/10.3133/ofr20231063>.

ISSN 2331-1258 (online)

## Contents

Abstract.....	1
Background and a Brief History.....	1
Clathrate Synthesis by a Novel Method—A Research Breakthrough.....	3
Making Fully Dense Clathrate Hydrates by Compaction.....	5
Results and Accomplishments.....	8
Result 1. Pioneering Cryogenic Scanning Electron Microscopy of Clathrate Hydrates.....	9
Result 2. CO <sub>2</sub> Clathrate; Synthesis, Phase Relations, and Equations of State.....	11
Result 3. Crystallography: Confirmation of sI and sII Crystal Structures and Discovery of High-Pressure Methane Clathrate Forms.....	11
Result 3a. Discovery of New Crystalline Forms of Methane Clathrate at Pressure.....	11
Result 4. Strength and Rheology of Compacted sI Methane Clathrate.....	11
Result 5. Adiabatic Elastic Properties of Fully Dense sI and sII Clathrates.....	12
Result 6. Thermal Properties of Porous and Fully Dense sI Methane Clathrate.....	12
Result 7. Decomposition Rates of sI Methane Clathrate and Other Clathrates.....	13
Result 8. Dissolution Rates and Stability of Lab-Made Clathrates Transported to the Monterey Canyon Seafloor.....	15
Result 9. X-ray Computed Tomography of Hydrate-Sediment Aggregates.....	15
Result 10. Chemical Exchange of Chlorofluorocarbons with Methane Clathrate.....	15
Result 11. Chemical Exchange of Noble Gases with Hydrocarbon Clathrate Hydrates.....	16
Result 12. Electrical Conductivity of Pure Clathrate and Clathrate-Sediment-Fluid Mixtures.....	16
Result 13. Characterization of Gas Hydrate Reservoir Sediments.....	17
Closing Remarks: Where to From Here?.....	18
Research Partners, Affiliations, and Funding Sources.....	19
Special Acknowledgments.....	20
Appendix 1. Evolution of the Seed-Ice Reaction Model to Form Pure Methane Clathrate.....	22
Appendix 2. Annotated Publication List.....	24

## Figures

1. A portion of the GHPL in Menlo Park in 2019.....	2
2. Methane hydrate samples created in our laboratory.....	3
3. Images from our laboratory featured on the cover of the journals Science and Science News, 1996.....	4
4. Diagram of our gas hydrate synthesis apparatus adapted for in situ uniaxial compaction and measurement of acoustic wave speeds.....	6
5. Diagram of thermal property apparatus with compaction capability.....	7
6. The custom triaxial deformation apparatus originally housed at Lawrence Livermore National Laboratory, adapted for cryogenic use.....	7
7. Cryogenic scanning electron microscopy, in use.....	10
8. Cryo-SEM images of natural gas hydrate and hydrate-bearing sediment.....	10
9. Photomicrographs of pure, polycrystalline CO <sub>2</sub> hydrate, originally synthesized and imaged in 2001 by methods described in Circone and others, 2003.....	10

10. Indium-encapsulated composite sample of methane hydrate and ice after deformation.....	12
11. Schematic diagram of our clathrate-synthesis pressure vessel, equipped with four internal thermocouples, connected to our flow-meter apparatus.....	13
12. Thermal map showing the “anomalous preservation” window .....	14
13. Photographs of the Monterey Bay Aquarium Research Institute remotely operated vehicle <i>Ventana</i> and clathrate samples placed on the seafloor offshore Monterey Bay, California .....	15
14. Working in the GHPL .....	16
15. Diagram of our custom-designed electrical conductivity apparatus and photomicrographs of polycrystalline test materials .....	17
16. Plots of a drillcore profile and photomicrographs of diatoms from a high-porosity layer in the core .....	18

## Tables

1. Summary of our clathrate research grouped by publication number .....	8
--	---

## Abbreviations

°C	degrees Celsius
µm	micrometer (or micron)
ACS	American Chemical Society
CCS	carbon capture and storage
CFC	chlorofluorocarbon
CH <sub>4</sub>	methane
CO <sub>2</sub>	carbon dioxide
CSEM	controlled-source electromagnetic
CT	computed tomography
cryo-SEM	cryogenic scanning electron microscope (or microscopy)
$\rho$	density
D <sub>2</sub> O	heavy water
DOE	Department of Energy
EM	electromagnetic

g	grams
g/cm <sup>3</sup>	grams per cubic centimeter
GHPL	Gas Hydrate Properties Laboratory
GHSZ	gas hydrate stability zone
GPa	gigapascal
K	Kelvin
LLNL	Lawrence Livermore National Laboratory
LN	liquid nitrogen
MBARI	Monterey Bay Aquarium Research Institute
MPa	megapascal
NASA	National Aeronautics and Space Administration
ORNL	Oak Ridge National Laboratory
P-T	pressure and temperature
Pa	Pascal
ROV	remotely operated vehicle
SEM	scanning electron microscope (or microscopy)
SIO	Scripps Institution of Oceanography
sl	structure I hydrate
sII	structure II hydrate
sH	structure H hydrate
THF	tetrahydrofuran
USGS	U.S. Geological Survey





# Summary of the History and Research of the U.S. Geological Survey Gas Hydrate Properties Laboratory in Menlo Park, California, Active from 1993 to 2022

Laura A. Stern and Stephen H. Kirby

## Abstract

The U.S. Geological Survey (USGS) Clathrate Hydrate Properties Project, active from 1993 to 2022 in Menlo Park, California, stemmed from an earlier project on the properties of planetary ices supported by the National Aeronautics and Space Administration's (NASA's) Planetary Geology and Geophysics Program. We took a material science approach in both projects, emphasizing chemical purity of samples, having controlled grain size and grain texture, and having verified crystal structures and phase relations. A foundational contribution from our USGS Gas Hydrate Properties Laboratory (GHPL) was in demonstrating the ability to reproducibly create such pure clathrate hydrate samples for study. Clathrate sample synthesis was achieved by heating sieved and weighed pure granular water ice in the presence of cold clathrate-forming gas or liquid. During heating, the ice melts at the grain scale and reacts with the gas to form clathrate. The resulting material has the desired uniformity and purity, with known intergranular porosity; our subsequent measurements showed that these clathrates exhibited the established clathrate structures and phase relations. This novel synthesis method was successful in creating clathrates of pure methane, ethane, propane, carbon dioxide, and multi-component gases. By mixing sand or silt with granular ice, we were also able to make clathrate-sediment aggregates with controlled grain textures. This simple method, adopted by many others in the community, permitted us to measure the physical and chemical properties of well-characterized and well-crystallized clathrates and clathrate/sediment aggregates. At about the same time, we adapted conventional scanning electron microscopy to cryogenic conditions for analysis of grain-scale characteristics of clathrates made in the GHPL as well as those collected from nature by drill core. The uniformity and reproducibility of our samples also allowed us to investigate how clathrates respond to environmental changes in chemistry, temperature, and pressure: we measured chemical exchange rates with dissolved gas species—such as noble gases and chlorofluorocarbons—as well as rates of clathrate dissolution and decomposition. These advances include the first accurate mapping of the conditions that promote the remarkable process of “anomalous

preservation” at room pressure, a metastability that offers potential application for low-cost and safe transportation of natural gas from gas fields far from pipelines.

Another advancement stemming from the GHPL was the compaction of as-synthesized porous clathrates to nearly full density by applying external pressure using three different techniques. Compaction allows for high-accuracy measurements of many fundamental physical and chemical properties of these materials, such as elastic wavespeeds and moduli, complete thermal properties, decomposition rates, thermal expansion, and clathrate equations of state. These properties and others, in turn, have helped USGS scientists to interpret geophysical well logs and active geophysical surveys, as well as model the rates of gas production from hydrate deposits in nature.

Studying this class of icy minerals that occur in abundance on Earth and in the outer solar system has been a fascinating laboratory journey. Here, we summarize the history and major findings of the USGS GHPL in Menlo Park, including both in-house research as well as findings from the synergistic collaborations with other agencies and institutes that were key to the success of our laboratory. The Menlo Park GHPL was more formally incorporated within the USGS Gas Hydrates Project, a collaboration among multiple USGS Science Centers, in the early 2000s under the leadership of Deborah Hutchinson, and now under the leadership of Carolyn Ruppel and Timothy Collett.

## Background and a Brief History

With the U.S. Geological Survey (USGS) moving many functions from Menlo Park, California, to the National Aeronautics and Space Administration's (NASA) Ames Research Center at Moffett Field in Mountain View, Calif., in 2021–2022, the USGS Gas Hydrate Properties Laboratory (GHPL) in Menlo Park has closed its doors. This concluding event is an opportunity to celebrate nearly three decades spent studying these fascinating compounds, and to take stock of additional insights and connections that become clear only after reviewing the GHPL's range of endeavors with its numerous partners.

## 2 Summary of the History & Research of the USGS Gas Hydrate Properties Laboratory in Menlo Park, Calif.

Clathrate hydrates, also called gas hydrates, are naturally occurring minerals on Earth and in the outer Solar System and are potential natural-gas resources for the future. Clathrate hydrates are crystalline solids consisting of hydrogen-bonded water molecules that form cage-like structures incorporating gas molecules of specific sizes within them, and form where temperature, pressure, and sufficient gas (and water) supply combine to make them stable. They typically form as structure I (sI) or structure II (sII) depending on composition and formation conditions, or more rarely as structure H (sH). On Earth, natural gas hydrate is most commonly sI methane hydrate.

The GHPL in Menlo Park was founded by S. Kirby and L. Stern in 1993 at the urging of Mary Lou Zoback, the then Director of the USGS Earthquake Science Center, to exploit an opportunity for the USGS to expand its NASA-supported research capability of measuring physical properties of planetary ices to include hydrocarbon clathrate hydrates. Kirby and Stern's early work on clathrate hydrates was also performed with long-time collaborator William Durham, then at nearby Lawrence Livermore National Laboratory (LLNL). Because methane hydrate is stable only at elevated pressures and low temperatures, laboratory research systems must be specially constructed in order to form gas hydrate as a pure phase (see for example, [Appendix 1](#)), and then preserve that hydrate while measurements are being made. In the beginning, we operated on a shoestring budget, using kitchen pots and pans and mostly second-hand instruments acquired on U.S. Government surplus; but through time our workstation

evolved into a highly specialized laboratory in which nearly all experiments were made in apparatus that we custom designed, built, and calibrated in-house ([fig. 1](#)). Throughout the lab's lifetime we benefitted from the Menlo Park location, building research ideas through collaborations with nearby research institutions, and building experimental systems through close communications with the USGS machine shops or with nearby commercial machine shops.

As our experience and collaborative network grew, so did opportunities to contribute more broadly to the growing community understanding of gas hydrate-related properties and processes. Our contributions completed with research partners resulted in 80 peer-reviewed papers from 1996 to 2022 ([Appendix 2](#)). These papers loosely track a research progression that begins with how gas hydrate can be reproducibly formed and characterized, moves through a collection of studies from our own lab on the properties and behaviors of pure gas hydrates, then branches into providing gas hydrate material for collaborative study in other laboratories, as well as in seafloor settings where it can form naturally. Interwoven with these studies is the description of analysis and imaging of gas hydrates formed either in our laboratory or retrieved from nature. In support of gas hydrate-community interest with respect to how gas hydrate interacts with its host sediment, we also created and tested mixed hydrate/sediment systems, and in related work, analyzed the host sediment itself from layers within, or bounding, natural gas hydrate reservoirs.

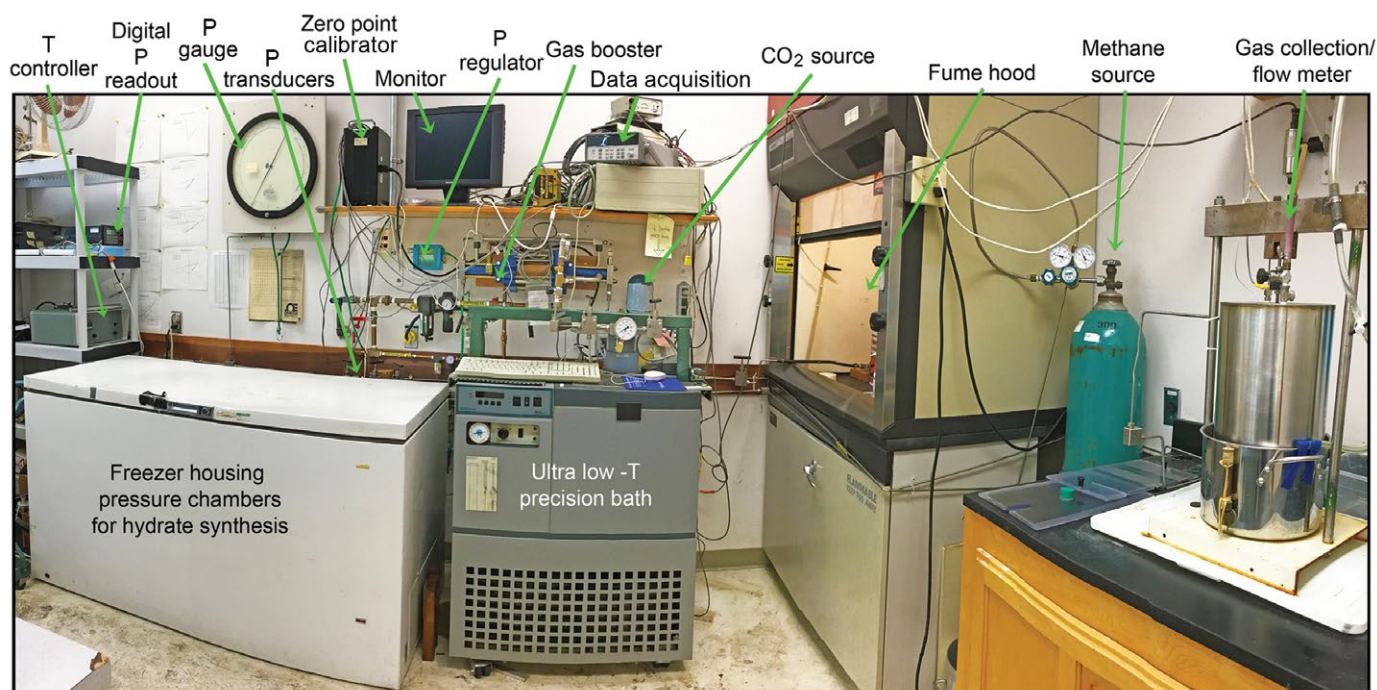


**Figure 1.** A portion of the GHPL in Menlo Park in 2019. The large freezer at left housed many of the apparatus described in this report. Also shown is the gas plumbing and boosting system, various instrumentation, and methane and carbon dioxide source tanks. The Hart ultra-low-temperature fluid bath enabled numerous experiments that required precise temperature resolution and accuracy. Our custom gas collection and flow-meter apparatus, shown at the far right, was used for all stability, dissociation, and stoichiometry experiments discussed in this report. Abbreviations: P, pressure; T, temperature. Photo: L. Stern.

Although our research topics evolved in response to community initiatives, opportunities, and collaborations, our contributions fundamentally relied on a commitment to sample characterization. Because gas hydrate is unstable at room conditions, establishing the purity of the gas hydrate and the arrangement of any other phases in the system (for example, gas, water, ice, salt, or sediment) is vital when running experiments in order to appropriately interpret results. From our initial studies on how to form pure gas hydrate, to culminating efforts in measuring the properties of hydrate/sediment/fluid mixtures, our most valuable results came when we allowed time to ensure full characterization of the materials under scrutiny.

## Clathrate Synthesis by a Novel Method—A Research Breakthrough

Our initial objective was to make pure, polycrystalline, clathrate hydrates of known and reproducible grain structure. We achieved this by reacting sieved, weighed, chemically pure, granular water ice grains, also called “seeds”, with hydrate-forming gases. The mixture was heated through the pressure-dependent ice-melting line, using a simple autoclave suspended in a fluid bath that was in turn housed in a commercial deep freezer. Reaction occurred primarily during the melting or “premelting” (a quasi-liquid film that can form on the surface of a solid even below its melting point) of ice along their grain surfaces. Full reaction, with no bulk-melting of the ice, was achieved by warming the reactants to temperatures deep within the hydrate stability field under high-pressure conditions. This unique method, later referred

to as the “seed-ice method,” allowed for verification of the completeness of the hydrate-forming reaction by detecting volume and enthalpy changes due to the melting and freezing of unreacted water, as those changes could be distinguished by pressure and temperature (P-T) anomalies while heating and cooling the sample through the ice-melting line. Fully reacted samples display no such P-T discontinuities. For methane hydrate, variable-sized polycrystalline sample masses of up to at least 100 grams (g) could be formed from 200-micrometer ( $\mu\text{m}$ ) seed ice grains packed in an autoclave, pressurized to 20–30 megapascals (MPa) methane pressure, during a single heating cycle to 15–17 degrees Celsius ( $^{\circ}\text{C}$ ), and typically accomplished overnight.

The resulting samples are remarkably cohesive despite their typical intergranular porosity of 20–30% (fig. 2). The initial pore space between the seed-ice grains diminishes as reaction progresses upon rearrangement of  $\text{H}_2\text{O}$  (water) molecules from their original ice  $I_h$  structure (hexagonal, with density  $[\rho] = 0.92$  grams per cubic centimeter  $[\text{g}/\text{cm}^3]$ ), to clathrate ( $0.78 \text{ g}/\text{cm}^3$  for an empty  $\text{sl}$  clathrate lattice), hence the resulting intergranular porosity can be pre-selected by how densely the (measured) ice seeds are packed into the constant-volume sample chamber. Late-stage clathrate crystallization at grain boundaries (discussed below) also improves competence and cohesiveness, rendering final samples that are easy to handle, store, transport, and shape for other purposes without crumbling.

In the mid-1990s, a critical limitation in gas hydrate research was access to well-characterized, pure gas hydrate material for study. Gas hydrate forms most rapidly at interfaces between  $\text{H}_2\text{O}$  and the hydrate-forming molecules

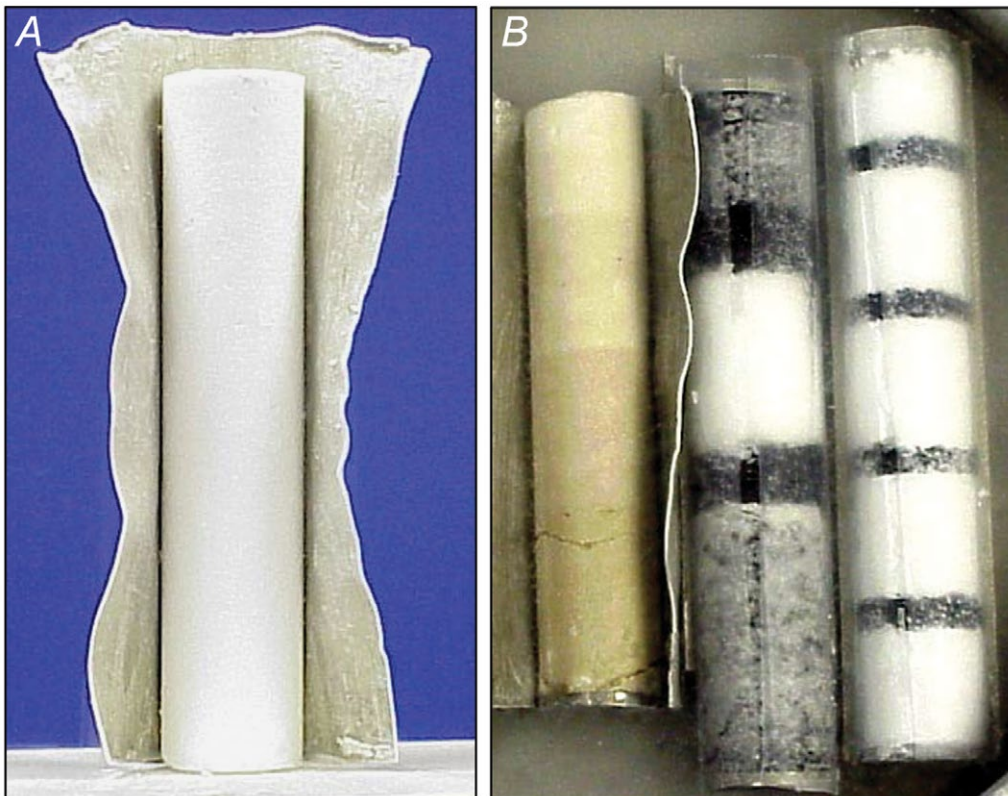


**Figure 2.** Methane hydrate samples created in our laboratory. *A*, Cylindrical test specimen of pure, polycrystalline methane hydrate. *B*, Mixed hydrate + sediment aggregates formed with pre-specified characteristics and known intergranular porosity. Samples are  $2.54 \times 10$ –11.5 centimeters. The leftmost two samples were grown in indium jackets, shown here split and peeled back. The two samples at the far right were grown in clear Teflon jackets, shown here split lengthwise along the upper surface. See Stern and others (2000) for further description of mixed-phase aggregate samples. Modified from figure 4 in Stern and others, 2000.

#### 4 Summary of the History & Research of the USGS Gas Hydrate Properties Laboratory in Menlo Park, Calif.

where H<sub>2</sub>O and the hydrate former are both concentrated. Hydrate formation at that interface, however, tends to segregate those molecules needed for further formation, dramatically slowing the formation rate. The success of our seed-ice method rests on those aspects that influence the availability of the hydrate-forming species at the growth front, in other words, those factors that influence diffusion rates, such as high pressure overstep, high temperature, high surface-to-volume ratio of the reacting grains, and small grain size, to minimize the volume of the unreacted core. The seed-ice method not only yields large volumes of hydrate in short formation times, but by observing the sample temperature during the cooling cycle, provides a means of assessing whether hydrate formation has run to completion with no excess or unreacted H<sub>2</sub>O. Our first publication on this method, and for that matter our first publication on clathrate hydrates in general, was selected for a 1996 cover report in *Science* (fig. 3; Stern and others, 1996). A quarter century later, that cover photograph showing a vibrant flame sustained by the resulting methane hydrate sample is the most frequently reproduced USGS hydrate image. Stern, Kirby, and Durham were invited to present a follow-up paper at the 1997 American Chemical Society (ACS) National Meeting in San Francisco, and for this they received the ACS Richard A. Glenn award for “Best Paper Presented in the Fuel Chemistry

Division.” The formal version of the Glenn award paper was published as the Keynote article for a special volume of *Energy & Fuels* (Stern and others, 1998a).

Our seed-ice method allows reproducible fabrication of clathrate samples that are chemically pure, free from unreacted ice, and mechanically cohesive. At the optical level, samples of pure clathrate are homogeneous from top to bottom (fig. 2A). Nevertheless, the specific process by which the ice completely transformed to hydrate remained uncertain—in particular, regarding the extent and effects of ice melting, a process that eluded detection in 1996 and that we deemed as possible evidence of short-lived superheated ice (Appendix 1). The postulation of superheated ice, in this context of clathrate formation above 0°C, in turn drew considerable interest for its potential insight into the dynamics of melt nucleation (see Pub. 1 in Appendix 2).

We further addressed our premise of superheated ice by investigating the clathrate growth process using multiple methods over the following few years. We first used a high-pressure optical cell—designed by I-Ming Chou (USGS), and with the assistance of our collaborator David Hogenboom (visiting from Lafayette College)—that appeared to support a “shrinking core” model of essentially solid-state reaction in which the rate of clathrate formation essentially keeps pace with incipient melting of ice, with no significant accumulation



**Figure 3.** Images from our laboratory featured on the cover of the journals *Science* and *Science News*, 1996. (Stern and others 1996. Photos: J. Pinkston and L. Stern.)

of melt even at temperatures above the ice-melting line (Stern and others, 1998b). However, we soon revised our model based on new information gleaned from improved thermal monitoring capabilities that showed definitive evidence for incremental melting. Concurrent experiments also revealed the high strength and low thermal conductivity of methane clathrate, helping to explain why the melting signature was previously masked. Lastly, after we acquired cryogenic scanning electron microscopy (cryo-SEM) capabilities in the early 2000s (discussed below in Result 1), direct, visual assessment of reaction textures exhibited by samples quenched at various stages of clathrate formation helped us improve our understanding of the clathrate-forming reaction. In addition to verifying a densely interconnected framework of polycrystalline methane hydrate in final samples, cryo-SEM revealed middle-to-late-stage crystallization of hydrate in pores and grain junctions where, presumably, small amounts of meltwater had migrated from nearby cores and was held in place by surface tension, where the residual water then reacts to form hydrate. The evolution of the ice-to-hydrate reaction model, including our original and revised interpretations of superheated ice, is chronicled by Stern and others (2004) and summarized in [Appendix 1](#).

Using the seed-ice method, we were also able to synthesize pure, porous forms of all the major hydrocarbon components of natural gas clathrates (methane, ethane, and propane) and carbon dioxide (CO<sub>2</sub>) clathrate, as well as heavy-water (D<sub>2</sub>O) clathrate deuterates. The heavier hydrocarbons—ethane and propane—required multiple overnight cycles, but still resulted in complete conversion of the ice reactant to form the clathrate hydrate product. Note that by “porous,” we refer to intergranular pore space; the clathrate grains themselves are fully dense. For CO<sub>2</sub> and propane clathrate, synthesis was more efficiently achieved by reacting ice with the clathrate formers in liquid phase rather than gas phase, but still resulted in final polycrystalline samples with uniform texture and stoichiometry.

Initially, concerns were voiced by some scientists that clathrates produced by our seed-ice method had different structure and properties from clathrates in nature, or those made by the traditional method of bubbling gas through cold gas-saturated water at high pressure to mimic nature. However, as described in this report, experiments showed that the seed-ice method results in clathrates that are structurally and chemically indistinguishable from those made using the previously established methods. Fundamentally, these concerns are about sample characterization, which has always been a focus for our lab. To characterize samples made using the seed-ice method, we measured and reproduced the published handbook P-T reaction lines and unit-cell parameters of sI and sII hydrocarbon clathrates and CO<sub>2</sub> clathrate hydrate as discussed in Results 2 and 3 below. Moreover, our clathrate samples were uniform from top to bottom ([fig. 2A](#)), indicating that melt water produced during the heating cycle was held in place by surface tension between ice and clathrate grains and did not sink by gravity flow to the bottom of samples.

Cryo-SEM imaging confirmed sample uniformity as well. Likewise, we were able to make reproducibly uniform, high-quality hydrate-sediment mixtures, or layered aggregates, by mixing sand or silt with granular ice and then heating these mixtures, at pressure, through the ice melting line ([fig. 2B](#)). Also, for the first time, we measured to three significant figures the hydrate number,  $n$ , the molecular ratio of water to gas, along the methane hydrate equilibrium curve and under other P-T conditions. These and related topics are chronicled later in this report (see “[Results and Accomplishments](#)”).

## Making Fully Dense Clathrate Hydrates by Compaction

For making fundamental physical property measurements on clathrates, it is often desirable to fully compact porous samples to eliminate intergranular porosity and its potential effects on properties. We did this using three different compaction methods in custom-designed-and-built apparatus:

1. Compacting using a double-acting hydraulic press adapted to working at freezer temperatures and inside a pressure vessel ([fig. 4](#)). “Double-Acting” means that by making valve changes, hydraulic pressure can be made to move the piston down (thereby compacting the sample by applying an axial compressive stress) or up (thereby reducing pressure on the sample). It also allows for the use of a displacement transducer, a dial gage and micrometer head on the exposed top end of the compaction piston; we could thereby measure the length change of the sample during compaction. After synthesizing porous clathrate by the seed-ice method directly within the compaction apparatus, we densified the sample by hydraulically advancing the top piston. Pore-space gas was vented through slits cut through the Teflon tubing that served as the sample jacket. Further description is provided in this report (see section “Result 5”).
2. A standard technique for measuring thermal conductivity and other thermal properties is by use of a needle probe ([fig. 5](#)). This method heats a cylindrical sample with a metal-sheathed probe located in an axial hole in the sample. By passing an electrical current through a heater wire loop that runs the length of the probe, the sample is heated. Temperature is measured by a thermistor junction that is co-located in the probe at its midpoint. The hydrate sample was made by the seed ice method described above and is jacketed using thin-walled Teflon tubing. The cylindrical sample was compacted radially by raising the fluid pressure in the annular space between the jacketed sample and the pressure-vessel wall and allowing gas in the sample pores to vent through a hole in a steel cylinder above the sample ([fig. 5](#)).
3. In 1976, Hugh Heard (LLNL) and Steve Kirby were funded by NASA to design and build a unique ice-deformation apparatus capable of deforming samples

## 6 Summary of the History & Research of the USGS Gas Hydrate Properties Laboratory in Menlo Park, Calif.

at temperatures as low as 77 kelvin (K, or  $-196\text{ }^{\circ}\text{C}$ ) and argon gas confining pressures up to 1 gigapascal (GPa). Shortly after the apparatus was built, colleague Bill Durham was hired by LLNL. He greatly refined and automated the control and data acquisition of this apparatus, allowing him to measure efficiently the strength and rheology of high-pressure polymorphs of water ice and many other icy compounds that are presumed to exist on the icy moons of the outer Solar System. Among these icy compounds were clathrate hydrates of natural gases. This radial compaction method results in nearly pore-free samples for subsequent determination of inelastic strength and rheological flow laws (fig. 6; see also Durham and

others, 2003, 2005, and references therein). Our productive collaboration with Bill on planetary ices continues to present day.

Our success at making pure, well-characterized clathrate hydrates attracted the interest of other laboratories, such as several U.S. Department of Energy (DOE) National Laboratories, university labs, and private research institutes. Our cooperative research was also facilitated by using liquid-nitrogen (LN)-cooled dewars to stabilize and transport clathrates made in the GHPL. For nearby laboratories we transported our samples by car in conventional LN dewars. For more distant labs, we were able to ship samples in specialized LN dry-vapor dewars approved by the U.S. Department of Transportation.

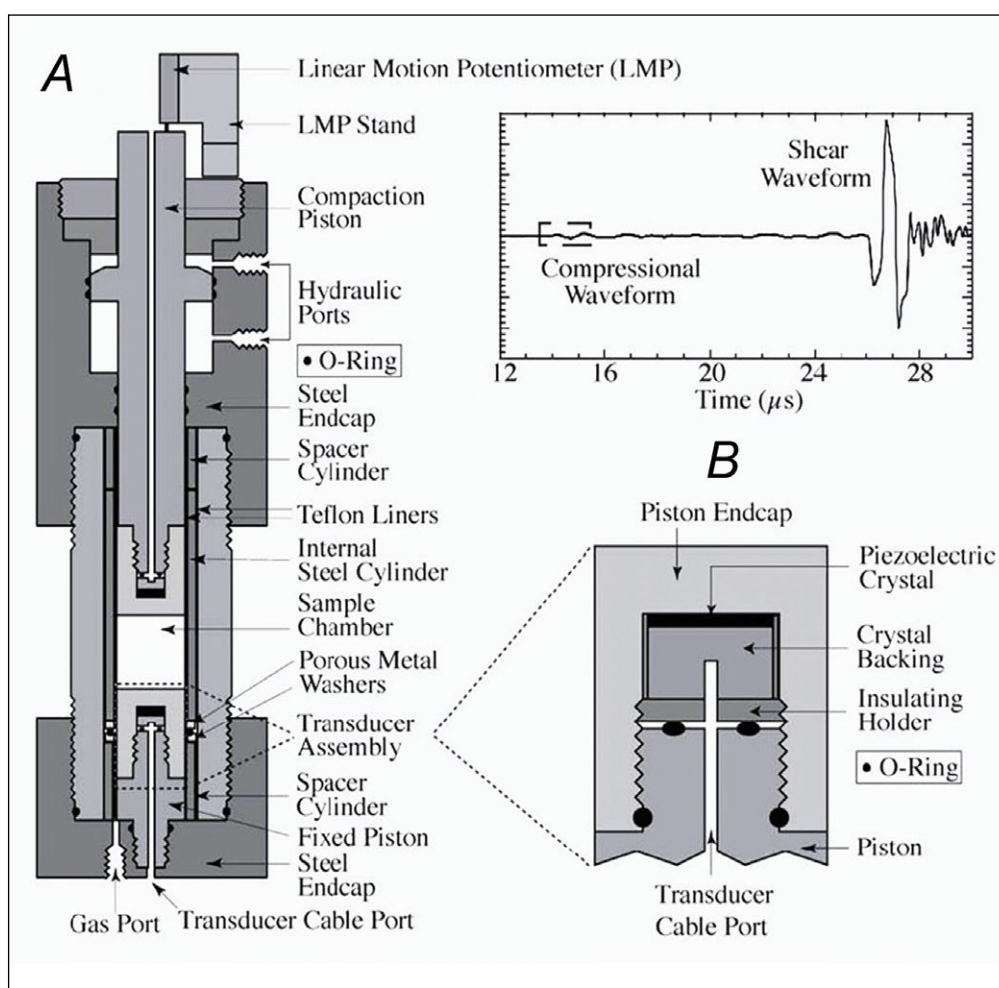


**Figure 4.** Diagram of our gas hydrate synthesis apparatus adapted for in situ uniaxial compaction and measurement of acoustic wave speeds (Waite and others, 2000; Helgerud 2001, Helgerud and other 2003a,b; Helgerud and others, 2009). *A*, Pressure vessel schematic. Polycrystalline gas hydrate is formed directly in the sample chamber by the seed-ice method and then compacted by hydraulically advancing the upper piston. *B*, Transducer assembly schematic. Both pistons house a 1-megahertz center-frequency piezoelectric transducer (either compressional or shear wave), allowing pulse-transmission wave-speed measurements to be made during the experiment. Abbreviation:  $\mu\text{s}$ , microsecond.

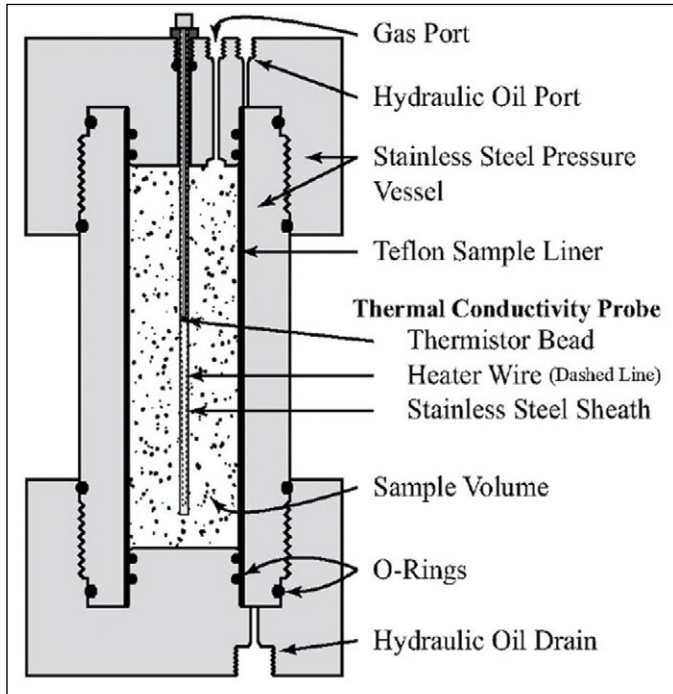


**Figure 5.** Diagram of thermal property apparatus with compaction capability, described by Waite and others (2007).

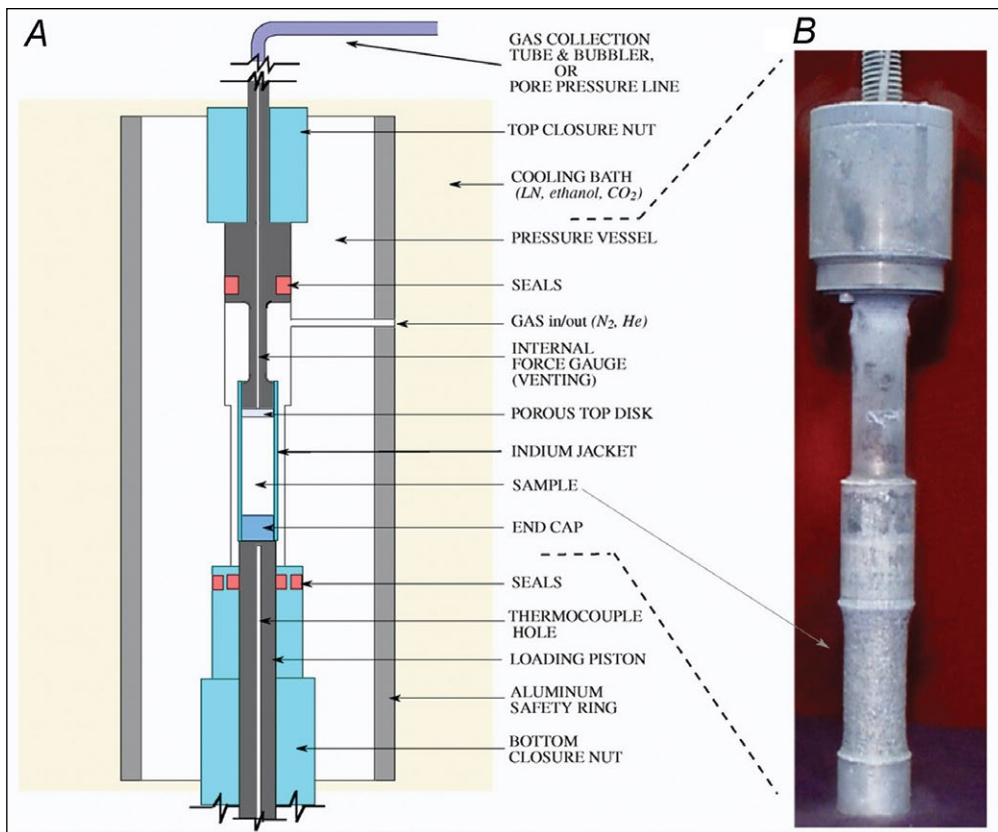


**Figure 6.** The custom triaxial deformation apparatus originally housed at Lawrence Livermore National Laboratory, adapted for cryogenic use. The full assembly is diagrammed in A. B shows an indium-encased pure methane clathrate sample attached to the venting force gauge through which pore-space gas can be eliminated (see Durham and others, 2003a,b). Photo by W.B. Durham. Argon (or, later, N<sub>2</sub> or He) gas is pressurized outside the indium jacket, thereby squeezing and compacting the sample. Abbreviations: CO<sub>2</sub>, carbon dioxide; He, helium; N<sub>2</sub>, nitrogen gas; LN, liquid nitrogen.

## Results and Accomplishments

Starting with pure clathrate hydrates made by these methods, we investigated a number of physical properties of these compounds to great accuracy in both porous and fully compacted forms. In choosing properties to target, we strove to address fundamental knowledge gaps the community identified for applied efforts, such as providing the mechanical and electrical property data to support remote detection of gas hydrate in nature, or the thermal and dissociation rate properties used in reservoir modeling efforts to assess the efficacy of recovering natural gas as a potential energy resource. The properties we measured, often community firsts, included strength and rheology, hydrate dissociation and dissolution rates, elastic wave speeds and elastic moduli, thermal conductivity, thermal diffusivity, heat capacity, electrical conductivity, and their temperature and pressure derivatives. To further test the quality and reliability of our measurements, we typically re-determined the physical properties of pure water ice  $I_h$  using identical methods and retrieved its established handbook values.

To reiterate, our approach has been to follow a materials science strategy for testing lab-synthesized materials. We consequently followed three precepts: (1) Know what you make by conducting macroscopic and microscopic

examination and characterization of the product, and by determining the crystal structure, including assessment of the degree of homogeneity. (2) Examine the samples after making physical and chemical property measurements to assure that the measurements themselves have not altered the structure or texture of the sample. (3) When possible, test the accuracy of results by measuring the properties of a standard material for which properties are well known with small measurement variance. Our standard was ordinary water ice  $I_h$ .

All told, we, along with our research partners, produced 80 gas-hydrate-property papers in peer-reviewed journals, books, and graduate theses over a period of 26 years (Appendix 2). In addition, we wrote over 75 technical abstracts that were presented at national meetings or hydrate conferences. In the late 1990s and early 2000s, we were proud to host in our lab as employees: post-doctorates Sue Circone and Bill Waite, and graduate students Mike Helgerud and Brian deMartin. John Pinkston, our long-term lab-operations manager, helped design and build all of our custom experimental apparatus. Here, we briefly describe the specific clathrate hydrate research topics investigated directly within the GHPL or in collaboration with others, and note their relevance and impact. In table 1, we organize and link our publications by subject matter and clathrate composition.

**Table 1.** Summary of our clathrate research grouped by publication number.

Research Topics and Partners	Publication no. (from Appendix 2)
Clathrate hydrate synthesis and formation processes from ice	
Synthesis of pure, polycrystalline, sI methane clathrate	1, 2, 3, 8
Synthesis of clathrate-sediment aggregate mixtures	8
Optical cell observation of formation processes, with D. Hogenboom	4
Synthesizing sI CO <sub>2</sub> clathrate	30
Synthesizing other clathrate compositions from liquid hydrocarbons	8, 35
Ice-to-clathrate reaction reevaluated at the sub-grain level	42
Crystallography and high-pressure phases	
Powder X-ray diffraction of methane clathrate and CO <sub>2</sub> clathrate	1, 3, 30
High-pressure phases of methane clathrate, with USGS colleague Chou	11, 12
Cell-structure and Rietveld, with ORNL partners Chakoumakos & Rawn	18, 21, 29, 30, 35
Crystal structure of methane-ethane clathrates, with LANL collaborator Tait	50
Clathrate stability, phase equilibria, stoichiometry, and dissociation kinetics	
Description of gas-collection and flowmeter apparatus	8, 13
Methane clathrate stoichiometry, decomposition, and stability	5, 8, 13, 37, 39, 40, 43, 44
Methane clathrate phase equilibria from thermodynamic calculations	51
Anomalous preservation of methane clathrate	8, 16, 17, 23, 24, 36, 38
CO <sub>2</sub> clathrate stability and dissociation behavior	30
sII methane-ethane clathrate stability	36, 50
Imaging	
Cryo-SEM imaging of lab-synthesized clathrates, including post-test materials	25, 31, 36, 39, 42, 45, 49, 57, 58, 67, 69, 72, 74, 77, 78



**Table 1.** Summary of our clathrate research grouped by publication number.—Continued

Research Topics and Partners	Publication no. (from Appendix 2)
Imaging—Continued	
Cryo-SEM imaging of natural gas hydrates	42, 48, 49, 53, 60, 65
Cryo- and conventional SEM imaging of gas-hydrate reservoir sediments	66, 68, 70, 71, 75, 76, 79
CT X-ray imaging of hydrates, with LBNL partners Kneafsey, Freifeld, Tomutsa	19, 26
Rheology and mechanical strength, with LBNL partner Durham	
Strength of pure methane clathrate	8, 31, 32
Strength of methane clathrate + sand, CO <sub>2</sub> clathrate, and sII clathrate	45
Thermal conductivity, diffusivity, specific heat, with GA Tech and USGS	
Pure, porous methane clathrate, with deMartin (then GA Tech) and Waite	14, 27, 28
Pure, compacted methane clathrate, with Waite (USGS)	52
Acoustic wave speeds $V_p$ and $V_s$ , with Helgerud (and Stanford advisors) and Waite	
Wave speeds in pure, compacted methane clathrate	9, 15, 33, 54
Wave speeds in pure, compacted H <sub>2</sub> O ice	34, 54
Wave speeds in pure, compacted sII methane-ethane hydrate	20, 33, 54
Gas hydrate measurements at the seafloor, with MBARI/USGS/LLNL team	
Dissolution measurements, with MBARI colleagues Brewer, Peltzer, Rehder	41
Deepsea testing of the CH <sub>4</sub> -CO <sub>2</sub> conversion hypothesis, with Brewer & Peltzer	63, 64
Guest-molecule exchange experiments, with SIO and USGS	
CFC uptake in hydrate, with SIO collaborators Kastner, Payten, Solem	22
Noble gas uptake in hydrate, with USGS colleagues Hunt, Ruppel, Pohlman	59, 61, 62
Electrical conductivity of pure sI methane hydrate	56, 57
Conductivity of methane hydrate + sediments + liquid water or brines	58, 67, 69, 72, 73, 74
Conductivity of pure sI CO <sub>2</sub> hydrate, and application to CO <sub>2</sub> sequestration	77, 78, 80

## Result 1. Pioneering Cryogenic Scanning Electron Microscopy of Clathrate Hydrates

An important complementary research direction of our clathrate synthesis method was the development of cryo-SEM to look closely at the structures of both lab-made samples and natural clathrates retrieved by drill core from marine sediments and permafrost settings (figs. 7, 8). This was made possible starting in 2001, with the acquisition of a cryogenic preparation station that attaches to the outside of the SEM and the integration of a cryostage into the evacuated SEM observation chamber. Cryo-SEM is typically used for materials that are not initially frozen (for instance, biological tissue or food science applications), so to successfully image clathrates and other icy compounds, we developed numerous sample-handling and imaging techniques to keep our materials cold and free from damage and condensation.

Acquiring cryo-SEM capabilities in the early 2000's was a game-changer for us by allowing grain-scale characterization of laboratory samples used in physical property tests as well as of hydrate-bearing samples retrieved from nature. Stern led this work and helped pioneer this sub-field of

clathrate research. With cryo-SEM, we confirmed that our lab-synthesized clathrates were remarkably reproducible and uniform. Spectacular cubic crystal forms of clathrates were often revealed along open cavities (see Front Matter image, also figs. 8.4, 9), further verifying that samples were well crystallized and lacked visible unreacted ice. Crystal faces often displayed fascinating details, such as etch pits, growth ledges, and growth mounds that were revealing of crystal growth processes. Importantly, cryo-SEM revealed that the seed ice hydrate-forming process was not a simple grain-for-grain conversion as we initially envisioned, but instead involved incremental melting of ice grain interiors as reported in Stern and others (2004) and summarized in Appendix 1. We later used X-ray fluorescence backscattered from the electron beam to identify the presence of key elements, such as carbon, critical for differentiating gas hydrate from water ice.

Cryo-SEM also provided a means to assess the morphology and distribution of other components in natural samples, including sediments and frozen fluids in addition to the gas hydrate itself. We used information gleaned from cryo-SEM not only for grain-scale characterization of site-specific natural gas hydrate in support of U.S. Geological

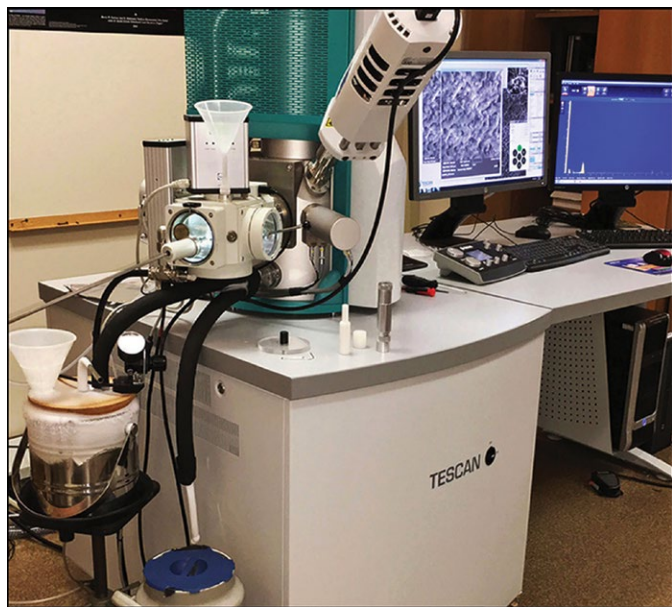


**Figure 7.** Cryogenic scanning electron microscopy (cryo-SEM), in use. Shown here is our Gatan ALTO1000 cryostage and preparation station attached to the Tescan variable pressure (VP) SEM housed at the U.S. Geological Survey Menlo Park campus from 2016 to present (2023). The system allows us to prepare and image samples down to  $-190\text{ }^{\circ}\text{C}$ . From 2001 to 2015, we used a Gatan ALTO2100 cryostage attached to a LEO field emission (FE) SEM. Photo by L. Stern.

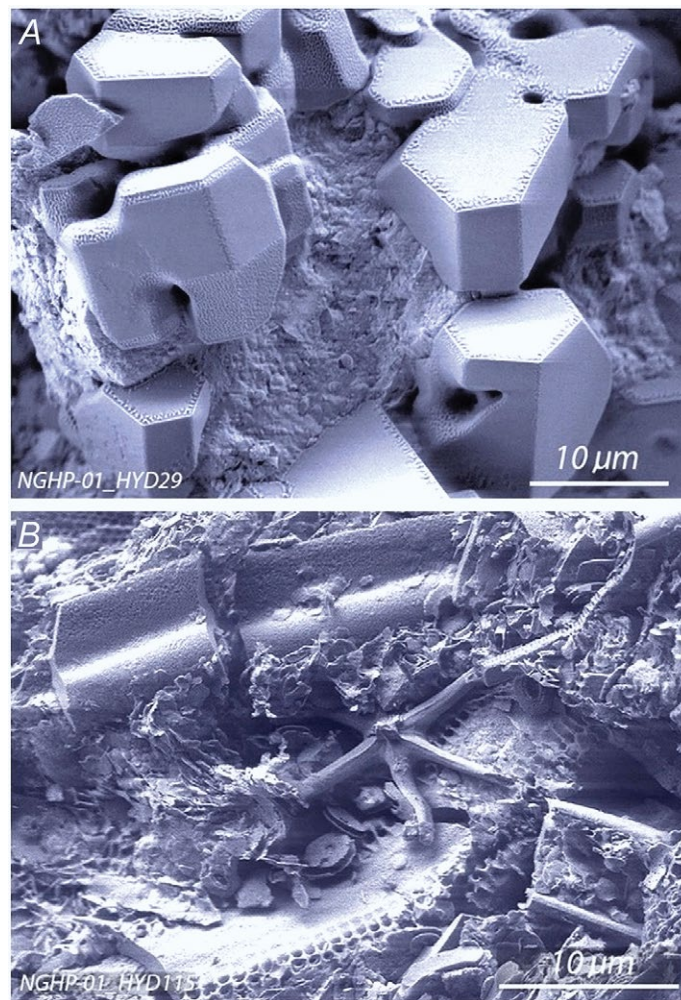


**Figure 8.** Cryo-SEM images of natural gas hydrate and hydrate-bearing sediment. Although few samples from nature display highly faceted crystal growth, several from the Indian National Gas Hydrates Joint Program NGHP-01 Expedition (offshore India) revealed vug-like development of gas hydrate crystals anchored to sediments (A). Other cores, such as those from the Andaman Islands site, display fine sediments mixed with microfossils and volcanic ash, cemented by gas hydrate (B). Modified from Stern & Lorenson (2014). Abbreviation:  $\mu\text{m}$ , micrometer.

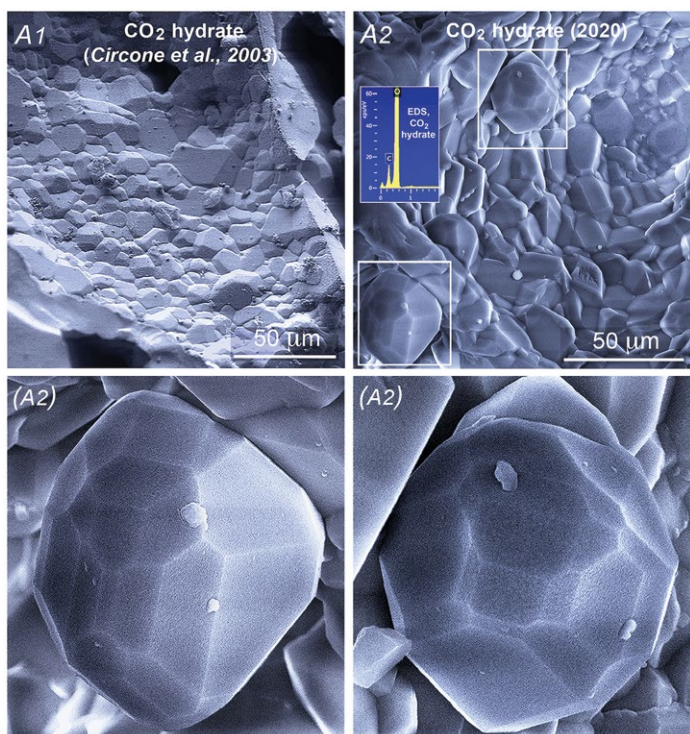


**Figure 9.** Photomicrographs of pure, polycrystalline  $\text{CO}_2$  hydrate, originally synthesized and imaged in 2001 by methods described in Circone and others, 2003 (A). The remaining portion of this sample was then wrapped in aluminum foil and stored undisturbed in liquid nitrogen (LN) for nearly 20 years prior to re-imaging in 2020 (A2) using the VP-SEM shown in figure 7. Two fully formed cubic crystals are outlined in A2 (note scale bar) and enlarged in the lower panels. In addition to revealing the crystalline development of the sample material, cryo-SEM allows for visualization of the effects of long-term storage; in this case, the sample retained at least most of its expected carbon content (note the energy dispersive X-ray spectroscopy plot with a carbon peak inset in A2) and, interestingly, suffered essentially no visible damage after two decades in LN. Modified from Stern and others (2021a,b). Photos by: S. Circone (A1), L. Stern (A2). Abbreviations:  $\mu\text{m}$ , micrometers.

Survey Gas Hydrate Project field operations, but also to help simulate natural textures when synthesizing gas hydrate samples in the lab for physical properties testing. Some of the natural gas hydrate samples that we assessed were recovered from marine environments such as from the NGHP-01 expedition offshore India, the Gulf of Mexico, and the Cascadia margin, whereas others included permafrost-related hydrates from the Mallik site in northwest Canada, and the Mount Elbert site on the Alaska North Slope (Stern and others, 2004; Stern and Kirby 2005, 2008; Stern and others, 2005a,b, 2011; Stern and Lorenson, 2014). In complementary work, we used cryo-SEM to address key questions relevant to sediment behavior in gas-hydrate-reservoir systems, described later in this report (Result 13).

From 2002 to 2014, we conducted cryo-SEM using field emission (FE) SEM operating under high-vacuum conditions (below  $10^{-5}$  millibar [mbar]), which, in turn, commonly caused sublimation and related surface damage to gas hydrate grain exteriors after approximately 20 minutes in the SEM column. Working expeditiously proved critical, as surfaces would otherwise develop a meso- or nanoporous appearance, leading to speculation by others that our lab-synthesized hydrates were not fully dense at the granular level. We demonstrated that the issue was entirely an artifact of the vacuum conditions and was not inherent to our hydrate synthesis process; an example is shown in figure 2 in Du Frane and others, 2015. After 2015, all cryo-SEM that we performed was with a newly acquired variable pressure (VP) SEM (fig. 7) in which column pressure was typically set to approximately 20 Pa ([pascals]; 0.2 mbar), and which fully eliminated the sublimation issue. In the VP-SEM, at sufficiently low temperatures, clathrate hydrate samples typically remain stable for more than 2 hours with little change in their appearance.

## Result 2. CO<sub>2</sub> Clathrate; Synthesis, Phase Relations, and Equations of State

Our motivation was to characterize some of the basic properties of CO<sub>2</sub> clathrate in anticipation of possible future uses for these data in efforts to sequester man-made CO<sub>2</sub> as CO<sub>2</sub> clathrate. This work, led by Sue Circone, involved learning to make pure, polycrystalline CO<sub>2</sub> hydrate samples, assessing grain morphology and characteristics (fig. 9), measuring stoichiometry number  $n$ , and determining stability behavior and decomposition processes (Circone and others, 2003). In related research, we formed the heavy water (D<sub>2</sub>O) version of CO<sub>2</sub> hydrate for a collaborative study on unit cell structure properties with Oak Ridge National Laboratory (ORNL) (see section “Result 3”). CO<sub>2</sub> hydrate samples were also used for rheological testing (section Result 4) and in ocean-floor dissolution experiments (Result 8). Lastly, we used our CO<sub>2</sub> hydrate synthesis method to form samples for electrical resistivity measurement (Result 12).

## Result 3. Crystallography: Confirmation of sI and sII Crystal Structures and Discovery of High-Pressure Methane Clathrate Forms

We assisted collaborators Bryan Chakoumakos, Claudia Rawn, and Adam Rondinone (all at ORNL) in obtaining lattice and cell structure data of several gas clathrate hydrates including methane, propane, and CO<sub>2</sub> clathrate. In Menlo Park, we developed methods to create heavy water (D<sub>2</sub>O) versions of these hydrates, which we synthesized directly into specialized vanadium canisters and shipped at liquid nitrogen temperature to our ORNL partners for neutron diffraction tests. This development permitted the deuterons to be precisely located in the crystal structures of the clathrates as hydrogen is difficult to locate by conventional X-ray diffraction methods. The resulting data, including Rietveld refinement, were used for fundamental crystalline characterization and resulted in five coauthored reports (Chakoumakos and others, 2002, 2003; Rawn and others, 2002, 2003; Circone and others, 2003). Importantly, the sharp diffraction peaks achieved by both neutron diffraction at ORNL, and X-ray diffraction at the GHPL, confirmed accepted sI and sII structures and verified the lack of contaminant phases such as ice. In a separate study, we hosted graduate student Kimberly Tait in the GHPL for crystallographic investigations of sI and sII methane-ethane hydrates (Tait and others, 2005).

### Result 3a. Discovery of New Crystalline Forms of Methane Clathrate at Pressure

Collaborating with USGS colleague I-Ming Chou and his associates on pressure-induced transformations in methane hydrate proved to be another successful study. This work resulted in identification of sII and sH structures of methane hydrate (Chou and others, 2001a), as well as a previously unknown high-pressure phase presumed stable in deep hydrate-bearing sediments underlying continental margins or in outer Solar System settings (Chou and others, 2001b). We provided the methane hydrate starting material required for diamond-anvil experiments.

## Result 4. Strength and Rheology of Compacted sI Methane Clathrate

A direct outgrowth of our long-term NASA research on planetary ices with Bill Durham were the first measurements of strength and rheology of pure methane clathrate. These tests were conducted on samples synthesized in the GHPL, then compacted and tested at LLNL using the apparatus shown in figure 6. A surprising result was that methane clathrate is markedly stronger and creep resistant than ordinary water ice (fig. 10), defying prior expectations, including even our own, that they were roughly similar in strength. Our earlier tests in the mid-1990s, on methane clathrate samples that developed ice within them during hydrostatic compaction procedures, indicated rheological behavior that was measurably—but not



**Figure 10.** Indium-encapsulated composite sample of methane hydrate and ice after deformation. Prior to our work with collaborator Durham at LLNL, gas hydrates were presumed to have ice-like strength characteristics owing to their H<sub>2</sub>O content and similarities in hydrogen bonding. Our results proved otherwise. This sample illustrates the dramatic strength contrast between ice (the bulging region) and methane hydrate (undeformed section labeled MH). This composite sample was a near-perfect cylinder prior to testing. The full sample was subjected to the same initial axial stress and radial pressure, but nearly all sample strain is accommodated by the significantly weaker ice portion. Compression direction is vertical (labeled  $\sigma_1$ ), and endcaps flank the sample at top and bottom. Modified from fig. 1 in Durham and others (2003a). Abbreviations: cm, centimeter.

significantly—stronger than pure water ice, a result we only later realized was due to the presence of the weaker ice phase itself. Improvements to our compaction methodology allowed us to then test pure methane clathrate, in turn revealing the enormous strength contrast between methane clathrate and water ice (Durham and others, 2003a, 2003b). This finding has important implications for loss of strength of hydrate-bearing formations if the hydrate is destabilized, which can affect seafloor geotechnical operations, drilling, platform stabilization, and seafloor slope stability. We then showed that while sI CO<sub>2</sub> hydrate and sII methane-ethane hydrate are also significantly stronger than water ice, measurable contrasts in strength exist between at least some sI and sII hydrates (for example sI methane hydrate compared with sII methane-ethane hydrate), and even between different compositions of same-structure hydrates (sI methane hydrate compared with sI CO<sub>2</sub> hydrate; Durham and others, 2005).

### Result 5. Adiabatic Elastic Properties of Fully Dense sI and sII Clathrates

This study was performed by Ph.D. student Mike Helgerud, postdoctoral fellow Bill Waite, and Stanford faculty advisors Amos Nur, Jack Dvorak, and Manika Prasad, all collaborating with our USGS team, in the GHPL. Using the double-acting hydraulic press fitted to a pressure vessel in

the GHPL (fig. 4, described earlier in “Making Fully Dense Clathrate Hydrates by Compaction”), the Helgerud-Waite duo measured elastic-wave speeds of compacted hydrocarbon hydrates at ultrasonic frequencies using shear-wave transducers incorporated into the bottom of the advancing (compacting) piston and in the top of the fixed piston under the sample (fig. 4). With the help of John Pinkston in reducing the electrical noise in the signal, the compressional wave signal naturally produced by the shear wave transducers could also be detected, meaning the team could simultaneously measure the acoustic travel times of both ultrasonic shear waves and compressional waves (fig. 4, upper right). Because we were able to measure these travel times and could accurately calculate sample length and therefore density, we could characterize the full adiabatic elastic properties of sI and sII hydrocarbon clathrates over a range of temperatures and pressures. Consistent with our laboratory’s verification strategy, the accuracy of these results was checked by measuring the fully dense elastic properties of ordinary water ice (as a standard with known elastic properties) in the same apparatus over a range of temperatures and pressures.

These were the first-ever acoustic measurements made on pure, end-member hydrocarbon hydrates. The well-established ice properties were reproduced within small experimental error, lending confidence to the accuracy of our reported clathrate elastic properties. These measurements have received much attention as they resulted in more reliable interpretations of well logs in hydrate-bearing sediments and improved interpretation of active-seismic field surveys in clathrate hydrate-bearing sediments (see Waite and others, 2000; Helgerud 2001; Helgerud and others, 2002, 2003a,b, 2009).

### Result 6. Thermal Properties of Porous and Fully Dense sI Methane Clathrate

The needle-probe method described earlier (fig. 5) allowed us to measure thermal conductivity,  $\lambda$ , of both porous (deMartin, 2001; Waite and others, 2002a, 2002b) and compacted (Waite and others, 2007) methane hydrate and ice I<sub>h</sub> over a range of pressures and temperatures. Needle probe measurements have been widely used to study marine sediments, but traditionally focus only on thermal conductivity. Changes in temperature recorded by the needle

probe thermistor during a thermal conductivity measurement are also controlled by a material's thermal diffusivity,  $\kappa$ , and heat capacity,  $c_p$ . Anticipating the response of natural marine occurrences of gas hydrate to thermal change, such as during methane extraction from hydrate as an energy resource, or hydrate breakdown owing to climate change in the shallow seafloor, thus requires knowing  $\lambda$ ,  $\kappa$ , and  $c_p$  for methane hydrate. The hydrate community had previously published results measured on mixtures of hydrate, ice or water, and methane gas, meaning corrections were commonly needed in order to recover the results for pure methane hydrate. Moreover, each property had been measured separately, and when taken together, the results did not obey the defining relationship,

$$c_p = \lambda / (\rho \cdot \kappa), \quad (1)$$

where  $\rho$  is the density of methane hydrate.

To address this knowledge gap, we worked to increase the data-acquisition rate during our needle probe measurements, which allowed us to make the first simultaneous measurements of  $\lambda$ ,  $\kappa$ , and  $c_p$  on compacted, pure

methane hydrate (Waite and others, 2007). We also extended our measurements to conditions above the ice melting line, making our measurements particularly relevant to conditions for natural marine occurrences of gas hydrates.

## Result 7. Decomposition Rates of sI Methane Clathrate and Other Clathrates

We conducted numerous experiments exploring gas hydrate composition and stability in the early to mid 2000s using our unique, custom-designed-and-built gas collection and flow-meter apparatus, based in part on the principles of a Torricelli tube (fig. 11). In this work, largely led by Sue Circone, we measured stoichiometry of methane hydrate, CO<sub>2</sub> hydrate, and sII methane-ethane hydrate over a range of pressure-temperature conditions, in addition to exploring annealing effects, phase stability, and dissociation kinetics that often varied considerably depending on the specific P-T path taken to remove the hydrate from its equilibrium stability field. In some cases, we used P-T paths analogous to those used in gas production scenarios from conventional reservoirs.

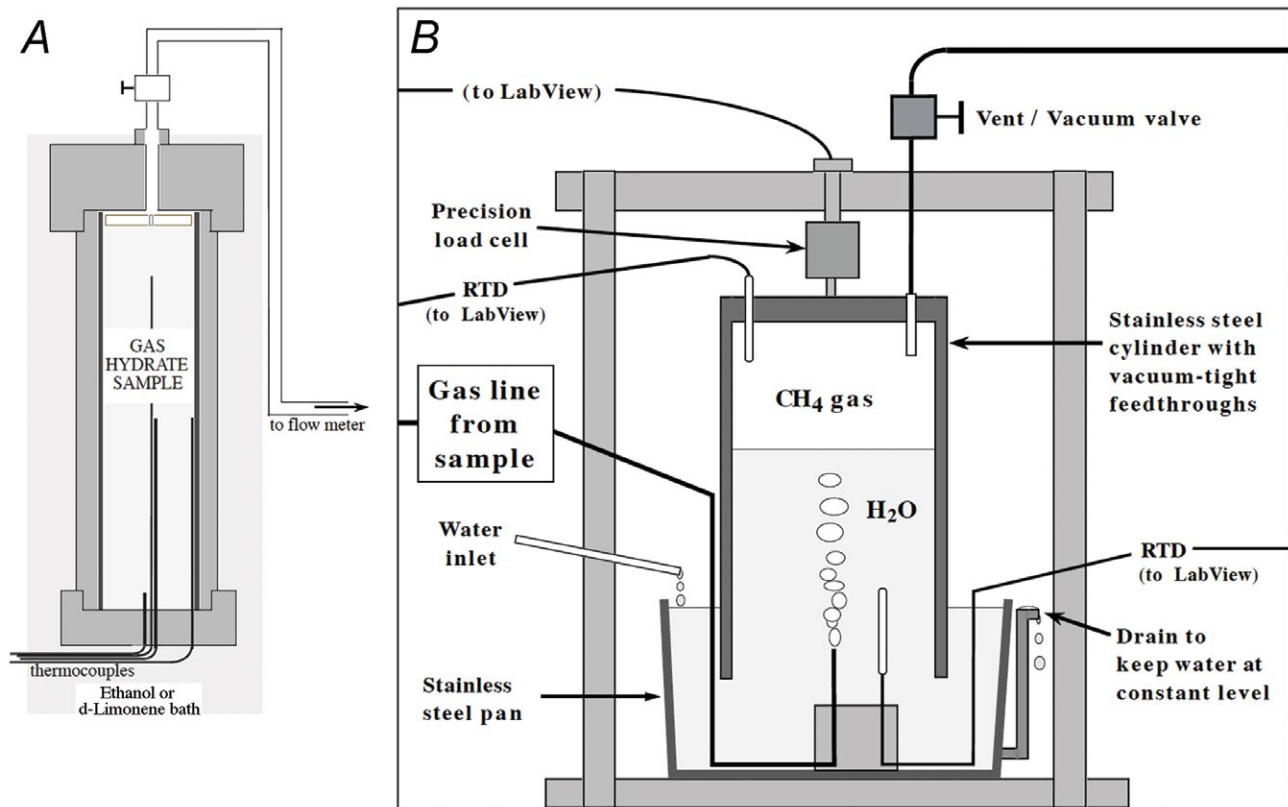


**Figure 11.** Schematic diagram of our clathrate-synthesis pressure vessel, equipped with four internal thermocouples (A), connected to our flow-meter apparatus (B). We designed, built, and used this system to monitor and collect methane, methane-ethane, or CO<sub>2</sub> gas released during dissociation experiments. By filling the inverted steel cylinder (shown in B) with water, then displacing the water by bubbling the dissociated gas into it, the precise change in weight of the cylinder measured the amount and rate of gas added to it. Gas volumes up to 7 liters (L) can be measured with an accuracy of about 15 milliliters (ml), and gas flow rates are measured over a range of 5 orders of magnitude. See Stern and others (2000) and Circone and others (2001, 2003, 2004a, 2004b) for further description. Abbreviations: CO<sub>2</sub>, carbon dioxide; L, liter; ml, milliliter; RTD, resistance temperature detector.

We also demonstrated that dissociation rates at pressure are controlled by the rate of heat flow into the clathrate, reflecting the endothermic nature of the decomposition. This reaction feature is one that makes ocean transporting of methane in the form of clathrate hydrate safer than transporting methane as liquefied natural gas (LNG), as it eliminates thermal runaway. In subsequent tests, we also measured sII methane-ethane clathrate decomposition rates. This work resulted in many publications: Circone and others (2000, 2001, 2003, 2004a,b, 2005a,b, 2006), Kirby and others (2004a,b), and Stern and others (2000, 2001a,b, 2002a,b, 2003).

A key discovery resulting from this effort was “anomalous preservation” of methane hydrate, a thermal window extending up to 75 degrees C above the expected dissociation temperature, where bulk quantities of metastable methane hydrate can be preserved for extended time—in some cases *months*—after rapidly releasing the gas pressure on the sample, in contrast to mere *minutes* when dissociated at low

temperature (fig. 12). This finding has important applications for the economic recovery and transport of methane hydrate due to the vastly improved accessibility offered by this thermal regime. Interest in our results came from academic and commercial research groups alike; our preservation method has been used in production processes for forming natural gas hydrate “pellets” for safely shipping natural gas and has application for recovery of natural gas hydrate by drill core. The discovery and “mapping” of the anomalous preservation regime (Stern and others, 2001a) remains our most highly cited work through at least 2023.

To close out our research on methane clathrate stability, Circone led a final study in which thermodynamic properties of phases in the  $\text{CH}_4\text{-H}_2\text{O}$  system were calculated from the Gibbs energy of reaction (Circone and others, 2006). The resulting thermodynamic model accurately reproduced published phase-equilibria data over a remarkably wide range of pressure-temperature conditions.

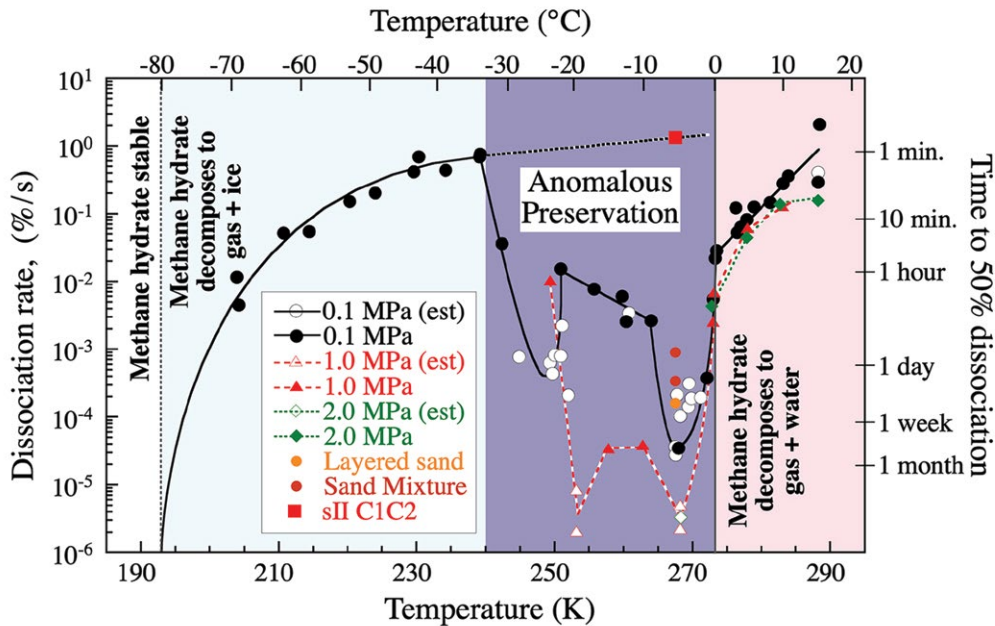


**Figure 12.** Thermal map showing the “anomalous preservation” window. Shown are decomposition rates for methane hydrate at various temperatures following rapid release of gas pressure to atmospheric pressure, or to 1.0 or 2.0 megapascals (MPa), in other words, outside of the methane hydrate equilibrium field. Each point represents a single isothermal experiment on one sample, showing the average rate (left axis) and time (right axis) that the “pressure-dropped” sample took to release 50% of its methane content. Rates become even slower during the second 50% of methane release. Importantly, dissociation rates in the anomalous preservation regime (purple area) are *orders of magnitude* slower than those extrapolated from lower temperature experiments (dotted curve). The longest preservation is achieved at only a few degrees below the ice melting point, where ice is quite weak. The accessibility of this regime, at atmospheric pressure, is what makes the preservation behavior so attractive for industrial applications related to natural gas transport. Above 0°C however, rates again steeply rise. Also of note is that while the addition of sand to samples only marginally affects the preservation effect, no comparable “preservation” of sII methane-ethane hydrate exists (red square near top of plot). See Stern and others (2001a,b, 2003) and Circone and others (2004b). Abbreviations: %/s, percent per second; C1C2, methane-ethane; est, estimated; K, Kelvin; MPa, megapascals.

## Result 8. Dissolution Rates and Stability of Lab-Made Clathrates Transported to the Monterey Canyon Seafloor

Working with ocean chemists Peter Brewer, Ed Peltzer, and their colleagues at the Monterey Bay Aquarium Research Institute (MBARI), we jointly made the first dissolution measurements of pure methane and CO<sub>2</sub> hydrate in undersaturated seawater in a natural ocean environment. Samples of methane hydrate, CO<sub>2</sub> hydrate, and later sII methane-ethane hydrate, were synthesized at the GHPL and in some cases compacted by colleague Bill Durham at LLNL. As a group, we designed a specialized vessel to transport these samples, under pressure, to 1,030 meters depth on the Monterey Canyon seafloor via MBARI's remotely operated vehicle (ROV) *Ventana* (fig. 13A). The ROV's "arms" were manipulated by the ship pilots to extract and position the samples for careful monitoring by high-definition television and time-lapse cameras (fig. 13B). Results demonstrated the large effects of seawater chemistry and flow patterns, in addition to gas solubility, on the longevity of hydrate on the ocean floor, and our data are used in prediction models for hydrate dissolution (Rehder and others, 2004).

A decade later, we partnered again with MBARI to undertake deep-sea (ROV-deployed) field tests monitored by in situ Raman spectroscopy to test the "spontaneous conversion" hypothesis that methane can be produced from

methane hydrate after injection of CO<sub>2</sub> by inducing swapping of the encaged molecules (and thus reforming solid CO<sub>2</sub> hydrate) with no liquid water production (Brewer and others, 2014a). Although such spontaneous conversion has been achieved in the laboratory, and moderate success demonstrated in field test sites (for example, Ignik Sikumi well, North Slope Alaska), our tests indicated that the dynamics and additional factors of the natural environment can complicate the replacement strategy and require further understanding (Brewer and others, 2014b).

## Result 9. X-ray Computed Tomography of Hydrate-Sediment Aggregates

We assisted Lawrence Berkeley National Laboratory colleagues Barry Freifeld, Tim Kneafsey, and Liviu Tomutsa in obtaining X-ray computed tomography (CT) images of sI methane hydrate-sediment aggregates inside a pressure vessel. These images demonstrate the first successful use of this technique to non-invasively differentiate gas hydrate from ice and the first images of a moving dissociation front (Freifeld and others, 2002, Tomutsa and others, 2002). This technique has since been used in arctic drilling projects for determining hydrate distribution in drill core material.

## Result 10. Chemical Exchange of Chlorofluorocarbons with Methane Clathrate

We performed this work with Professor Miriam Kastner (Scripps Institution of Oceanography, SIO) and her student Christian Solem, and Adina Payton (Stanford University, now at University of California, Santa Cruz). The occurrence of trace amounts of chlorofluorocarbons (CFCs) in naturally occurring gas hydrates motivated us to investigate exchange rates of manmade CFCs in seawater with laboratory-made methane hydrate. The ratio of CFC-11/CFC-12 in seawater is commonly used to calculate seawater's apparent age, and CFC-11 and CFC-12 have appropriate molecular diameters to occupy sI gas hydrate cages. If they incorporate into natural marine gas hydrates, could they be used to date seafloor

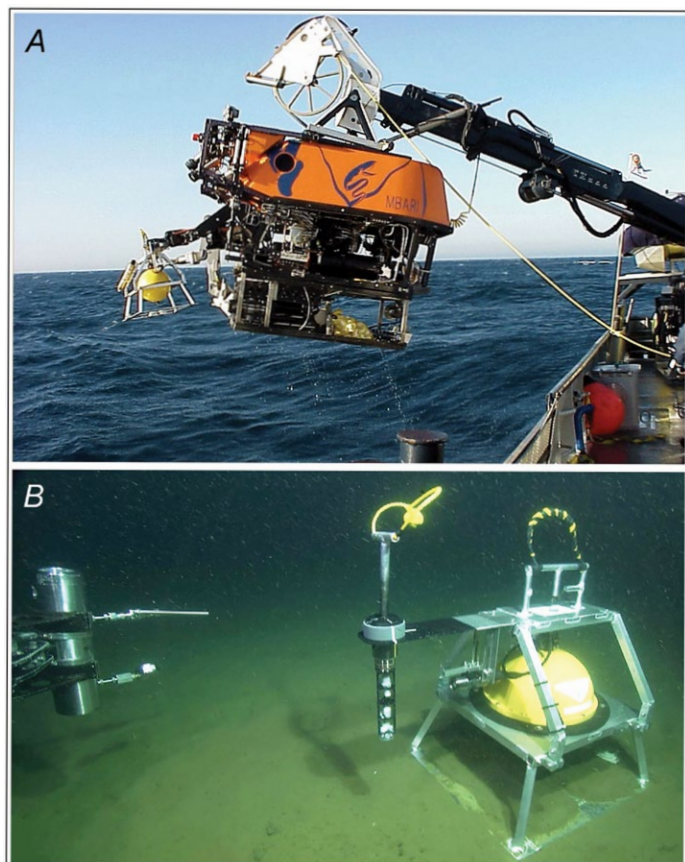


**Figure 13.** Photographs of the Monterey Bay Aquarium Research Institute (MBARI) remotely operated vehicle *Ventana* (A) and clathrate samples placed on the seafloor (B) offshore Monterey Bay, California. In this MBARI-USGS-LLNL team effort, samples of pure methane hydrate, CO<sub>2</sub> hydrate, and sII methane-ethane hydrate, all from the GHPL, were deployed to the ocean floor via the *Ventana* for measurement of dissolution rates at 1030-meter water depth. Upon reaching the site, the ROV robotic arms were maneuvered to unpack the pressure vessel containing the samples, depressurize and open the vessel, then remove the "hydrate hotel" from within and place it in the sample rack holder (B). Dissolution was monitored using time-lapse and high-definition video cameras (Rehder and others, 2004). Photos courtesy of MBARI.

and shallow sub-seafloor gas hydrates? We investigated this question by synthesizing gas hydrate samples using the seed ice method in the presence of a known methane plus CFC source gas, then analyzing the gas composition released by the resulting hydrate samples after venting all pore-space and head-space gas. In companion tests, we conducted multi-week exchange experiments. Results showed that CFC-11 and CFC-12 can indeed become incorporated within methane hydrate, both during formation and through subsequent exchange with ambient gas, in turn suggesting that hydrates may record the pore-fluid or bottom-water CFC concentration from which they were formed (Solem and others, 2002).

### Result 11. Chemical Exchange of Noble Gases with Hydrocarbon Clathrate Hydrates

Predicting the susceptibility of gas hydrates to warming climate is problematic owing to the difficulty in distinguishing between methane released from gas hydrate and methane released from other sources (seeps, coal beds, etc). Stern worked with others on the USGS Gas Hydrate Project (Andrew Hunt, Carolyn Ruppel, and John Pohlman) to investigate noble gas fractionation patterns associated with methane hydrate formation and dissociation as a means of “fingerprinting” the released gas. Samples were synthesized by Stern from specialty gas mixtures under high-pressure and low-temperature conditions, then subjected to treatments simulating aging, retrieval, handling, and storage of natural hydrates. We built a special apparatus in Menlo Park for careful step-wise collection of the evolving gas, which, in turn, was analyzed by Hunt at the USGS Noble Gas Laboratory in Denver for isotope composition, ratios, and fractionation effects. Natural gas hydrate samples were also tested for comparison. Our results confirmed a unique pattern, based in part on partitioning by molecular weight of noble gases, that shows potential as a fingerprint for hydrate-sourced methane emissions. (Hunt and others, 2011, 2013a, 2013b).

### Result 12. Electrical Conductivity of Pure Clathrate and Clathrate-Sediment-Fluid Mixtures

Electrical properties of pure methane hydrate had never been measured prior to our work yet they are needed to help quantify electromagnetic (EM) measurements from field surveys and for use in modeling efforts. Toward this goal, Stern partnered with Steven Constable of SIO, and Wyatt Du Frane, Jeff Roberts, and Ryan Lu at LLNL, from 2010 to 2021, under DOE funding, to determine electrical conductivity of methane hydrate and hydrate/sediment/fluid mixtures (figs. 14, 15). All experiments were conducted in the GHPL, using a custom-designed-and-built apparatus in which in situ measurements of impedance were made on samples formed by the seed-ice method (fig. 15A). The team reported the first-ever electrical conductivity measurements of pure, polycrystalline

methane hydrate (Du Frane and others, 2011a,b) and then quantified the effects of systematically adding sediment components and/or saline pore fluids to the system (Du Frane and others, 2011c, 2015; Lu and others, 2018, 2019; Constable and others, 2020a,b). After testing, all samples were imaged by cryo-SEM to assess grain characteristics and the connectivity of the various components (fig. 15B), in turn allowing evaluation of conduction mechanisms.

Our results demonstrated that pure methane hydrate can be distinguished from pure water ice by their electrical signatures, and also highlighted the important contribution of even minor impurities derived from sediment surfaces in addition to the large effects of salt-bearing phases (including seawater) on the electrical properties of mixed-component samples. But what about the composition of the guest molecule itself?

To address this final question, the team made the first conductivity measurements on pure CO<sub>2</sub> hydrate for direct comparison with pure methane hydrate, as both are sl



**Figure 14.** Working in the GHPL. Shown here is our lab-operations manager John Pinkston (left), with Lawrence Livermore National Laboratory collaborator Wyatt Du Frane (right), taking apart the electrical resistivity apparatus to retrieve a hydrate sample inside for cryogenic SEM analysis. Photo: L. Stern.



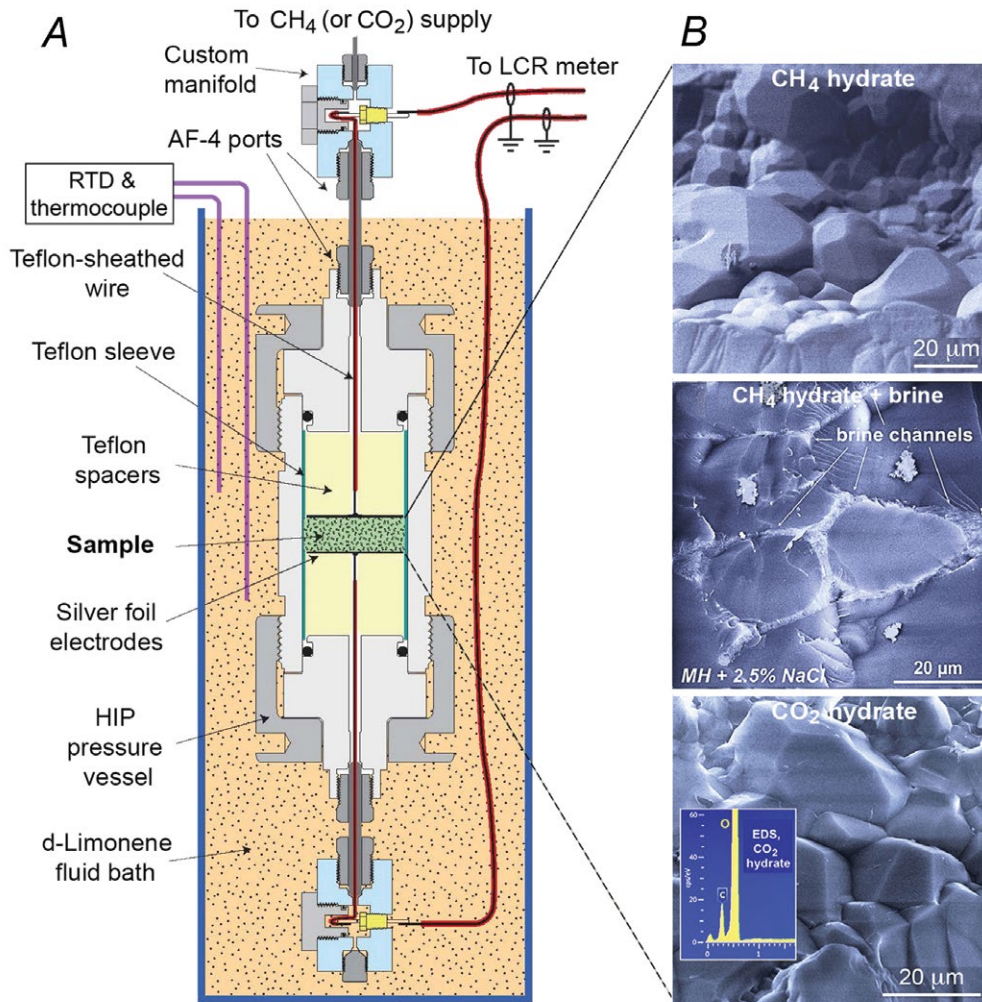


**Figure 15.** (A) Diagram of our custom-designed electrical conductivity apparatus (first described by Du Frane and others, 2011b), and (B) photomicrographs of polycrystalline test materials: pure methane hydrate, methane hydrate plus an interconnected saline fluid phase (now frozen in place), and pure CO<sub>2</sub> hydrate. Energy Dispersive Spectroscopy (EDS) scan shown as inset in (B) confirms the presence of carbon in addition to oxygen, in turn confirming that the imaged material is CO<sub>2</sub> hydrate, not ice. (Photos: L. Stern).

clathrates with near-identical cage filling. We discovered that they in fact exhibit measurably different electrical signatures, possibly owing to distortion of the small cages in CO<sub>2</sub> hydrate (Stern and others, 2021a,b). Although the significance of these results will take more time to evaluate, the distinct electrical signatures of CO<sub>2</sub> hydrate versus methane hydrate show promise for the use of EM methods in monitoring CO<sub>2</sub> hydrate formation or sequestration in certain natural, remote settings (described in “Closing Remarks”).

### Result 13. Characterization of Gas Hydrate Reservoir Sediments

In addition to assessing natural gas hydrate from marine and permafrost settings described in section “Result 1” above, Stern worked closely with USGS Gas Hydrate Project members in Woods Hole (William Waite, William Winters,

Junbong Jang) to establish the following: (1) grain-scale characterization and sediment properties of hydrate reservoir and bounding layers associated with targeted reservoirs from offshore India and from Ullung Basin sites offshore South Korea, (2) the effects of pore-fluid chemistry changes on fine-grained particles associated with reservoir sediments, and (3) the specific role of fine-grained sediment in creating pore-throat clogs during gas production (fig. 16). Cryogenic- and conventional SEM and related analyses were combined with index property, electrical sensitivity, and compressibility measurements of recovered sediments from select sites, as well as on lab standards for comparison (Winters and others, 2014; Jang and others, 2018a; 2019a,b,c; 2020a,b; 2022a,b,c). This work serves to establish physical properties of hydrate-bearing sediment layers and reservoir seals and yields insight into the specific and complicated effects of fine sediments during methane production scenarios.

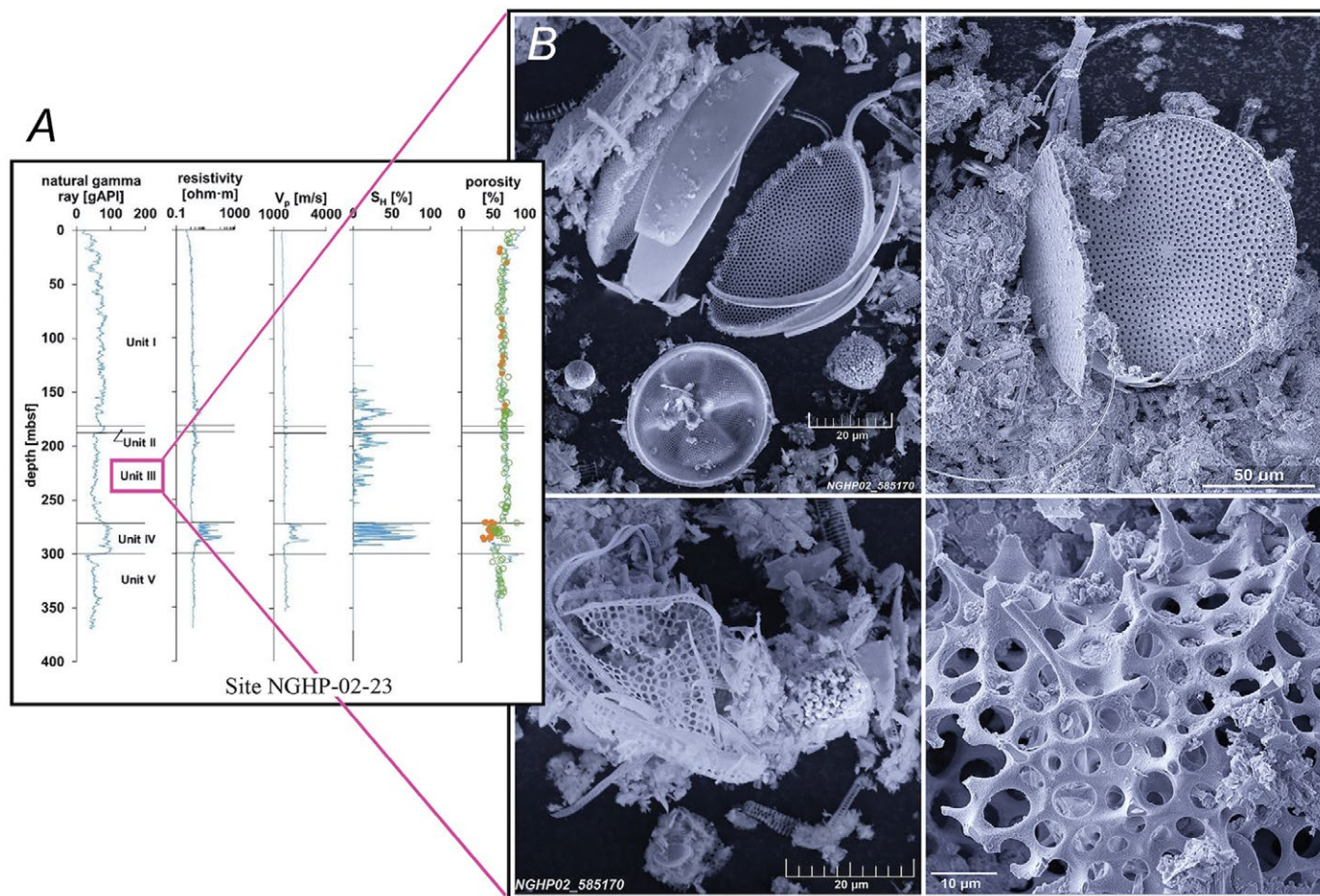


**Figure 16.** Plots of a drillcore profile and photomicrographs of diatoms from a high-porosity layer in the core. Scanning electron microscopy helps to address questions about lithologic control on gas hydrate occurrence and morphology. One example involved the examination of fine-grained sediments within cores from India’s NGHP-02 expedition. Panel A (modified from Jang and others, 2019a) shows a part of a well profile from site 23. Here, diatoms in lithologic Unit III (B) are largely responsible for the surprising increase in porosity with depth that reaches about 70% above its contact with Unit IV. Unit III lithology and porosity presumably allows fluid- and dissolved-phase methane to escape the underlying hydrate-bearing Unit IV and form gas hydrate in the fine-grained overburden. Shown in the well profile are natural gamma-ray activity (in API gamma ray units), resistivity (in ohm meters), compressional wave speed ( $V_p$ , in meters per second [m/s]), hydrate saturation ( $S_H$ ), and porosity listed by percent (%).

## Closing Remarks: Where to From Here?

The full spectrum of our work on clathrate hydrates is cross-correlated by subject matter, clathrate composition, and publication number, in [table 1](#). Reflecting upon this body of work as a whole, perhaps its most useful contribution lies in the consistency in utilizing, whenever possible, uniform protocols, materials, and methodologies for over 25 years, a theme first discussed in the early sections of this report. In turn, this now provides us with an unusually long-term and internally consistent compendium of results to draw from. For instance, methane hydrate and quartz sand aggregate mixtures made for strength tests in the early 2000s were formed by identical techniques, and from the same reactants and  $\text{SiO}_2$  particulate standards, as methane hydrate and quartz sand mixtures used in “anomalous preservation” and related dissociation experiments,

as well as those used in electrical conductivity experiments years later. Similarly,  $\text{CO}_2$  hydrate samples were synthesized from the same  $\text{CO}_2$  source tank over the years and using the same seed-ice preparation protocols (and water source) as methane hydrate, with the actual measurements themselves conducted in the same apparatus and monitored by the same instrumentation as methane hydrate test specimens. The uniformity also crossed over for samples undergoing neutron and (or) X-ray diffraction analysis, as well as those created for ocean-floor dissolution experiments. Testing the accuracy of all apparatus and methodologies by re-measuring and retrieving the known properties of pure water ice Ih provided further basis for reliable comparisons to be made over the years.

That is to say, when our experiments yielded unexpected results and surprises, or even nuanced, complex behavior, we could nearly always rule out sample preparation, handling, or

apparatus dependencies as being the culprit, which is typically difficult to decipher when comparing previous results from other laboratories. The GHPL's work also revealed clear instances where the specific structure of the hydrate phase proved of considerable consequence (for example, sI methane hydrate versus sII methane-ethane hydrate), as can different compositions of same-structure hydrate (for example, sI methane hydrate versus sI CO<sub>2</sub> hydrate, despite near-identical cage filling). Use of analogue materials such as tetrahydrofuran (THF) hydrate for example, or ice, misses such discernment.

Now that the GHPL is largely dismantled, how might this anthology be leveraged? We close this report with an example of reexamining the database as a whole, from the perspective of addressing increasingly urgent and topical issues—namely, carbon neutrality and carbon capture and storage (CCS) goals.

Two critical components for safe and reliable CO<sub>2</sub> sequestration in geological settings involve careful monitoring of injected CO<sub>2</sub> into the targeted region, and verifying the integrity of the repository, including reliable detection of possible leakage. Constable and Stern (2022; report no. 80 in [Appendix 2](#)) illustrate how controlled-source electromagnetic (CSEM) methods—currently used for oil and gas exploration, and exceptionally sensitive to electrically resistive structures—might effectively be used to monitor CO<sub>2</sub> sequestration in deep seafloor environments, and likely also extending to somewhat shallower settings related to the gas hydrate stability zone (GHSZ). Indeed, gas hydrates play numerous roles in CO<sub>2</sub> sequestration strategies in the marine environment; for instance, in forming a CO<sub>2</sub> hydrate “top cap” in deep seafloor environments that can effectively serve as a secondary sealing mechanism by greatly reducing dissolution of gravitationally-trapped liquid CO<sub>2</sub> below (reviewed in Constable and Stern, 2022). Alternatively, CO<sub>2</sub> can be stored as a solid hydrate phase itself in the GHSZ and is also of interest for possible CO<sub>2</sub>-for-CH<sub>4</sub> replacement processes in the GHSZ, a topic of active research as discussed earlier in section “Result 8.” Not only can laboratory measurements provide further insight into these various sequestration scenarios, but as modelling efforts continue to advance, so will the usefulness of increasingly well-constrained and better-informed input parameters.

With this in mind, Constable and Stern (2022) reexamined specific results from the GHPL where, over the span of many years, certain physical property differences were identified as distinguishing sI CO<sub>2</sub> hydrate from sI methane hydrate: most notably, strength, dissociation behavior, dissolution kinetics, and electrical conductivity (see Results 4, 7, 8, and 12). These factors may, in some cases, influence the monitoring strategy and even the stability of sequestered CO<sub>2</sub> in regions within or proximal to the GHSZ, possibly extending to site-selection itself. Our electrical property measurements, in particular, may help guide discussion on utilizing CSEM technology and related data inversions to address the safety-related monitoring concerns described above, including evaluation (in some cases) of possible breaches to a simulated CO<sub>2</sub> reservoir. Moreover, advances and insights gleaned from

recent work conducted in the GHPL may in some cases help resolve questions surrounding previous enigmatic results. For example, Constable and Stern (2022) note that the point-defect and lattice-imperfection factors implicated in the electrical property contrasts between CO<sub>2</sub> hydrate and methane hydrate (Stern and others, 2021a,b; see “Result 12”) are likely also rooted in other diverging responses that were difficult to explain at the time, such as the rheological contrasts between these same two sI hydrates measured by Durham and others (2005; see section “Result 4”).

Steve Kirby, now a USGS Scientist Emeritus, officially retired from clathrate research in 2011 but retained keen interest in ongoing GHPL research efforts and enjoyed consulting on various topics and equipment design. Laura Stern continued this research as Laboratory Chief through the end of 2021. Now also a retired emeritus scientist, she continues with cryogenic scanning electron microscopy (cryo-SEM) investigation of natural gas hydrates obtained by drill core in support of USGS Gas Hydrate Project field expeditions. As we close out our USGS Menlo Park laboratory efforts, we hope this overview provides a useful roadmap to our compendium of results, and that, over the years to come, the source papers themselves continue to provide quantitative and qualitative insights into laboratory and field applications.

## Research Partners, Affiliations, and Funding Sources

The success of our laboratory could not have been accomplished without the expertise and dedication brought by postdoctorates Sue Circone and Bill Waite and graduate students Mike Helgerud and Brian deMartin. Sue went on to teach Geology at Washington State University, Bill went on to lead the U.S. Geological Survey (USGS) Gas Hydrate Laboratory in Woods Hole, Mass., and Mike and Brian serve as senior-level supervisors at ExxonMobil. We also benefitted tremendously from support from within and outside the USGS. These partnerships and sources of support include:

- USGS Gas Hydrate Project past and current members from other USGS Science Centers:
  - o Coastal and Marine Geology, Woods Hole, Mass.: Bill Dillon (emeritus), Debbie Hutchinson, Carolyn Ruppel (project Co-Leader), Bill Waite, Bill Winters, David Mason, John Pohlman, and Junbong Jang (now a professor at Dong-A University).
  - o Energy, Denver, Colo.: Timothy Collett (project Co-Leader).
  - o Pacific Coastal and Marine Geology, Menlo Park and Santa Cruz, Calif.: Keith Kvenvolden (emeritus) and Tom Lorenson.
  - o Geology, Geophysics, Geochemistry, Denver, Colo.: Andrew Hunt.

- o USGS laboratory of I-Ming Chou in Reston, Va.: I-Ming Chou and Bob Burrus, along with Washington Geophysical Laboratory senior staff Russ Hemley and David Mao.
- Lawrence Livermore National Laboratory: Bill Durham (now Massachusetts Institute of Technology, MIT), Wyatt du Frane, Jeff Roberts (now University of California, San Diego), and Ryan Lu (now private sector).
- Monterey Bay Aquarium Research Institute: Peter Brewer, Ed Peltzer, and Gregor Rehder (then Postdoctoral Fellow, now at IOW [Leibniz Institute for Baltic Sea Research Warnemunde]).
- Scripps Institution of Oceanography (San Diego, Calif.): Steven Constable and Miriam Kastner.
- Stanford University Department of Geophysics: graduate student Mike Helgerud (now at ExxonMobil Upstream), Postdoctoral Fellow Bill Waite (now at USGS in Woods Hole, MA), and Professors Jack Dvorkin, Amos Nur, and Manika Prasad (now at the Colorado School of Mines, CSM).
- Lawrence Berkeley National Laboratory: George Moridis, Barry Freifield, Timothy Kneafsey, and Liviu Tomutsa.
- Oak Ridge National Laboratory: Claudia Rawn, Brian Chakoumakos and their research associates.
- Georgia Institute of Technology: Brian DeMartin (now ExxonMobil) during his Master's Thesis research, under advisor Carolyn Ruppel.
- Lafayette College: David Hogenboom. (Now retired.)

We are grateful for the numerous funding sources throughout the decades that provided support for us to build our lab, conduct our research, and acquire specialty instrumentation such as: cryostages for the SEM, an X-ray diffraction instrument equipped with a water chiller and designated computer, an ultra-low-temperature chest freezer, a precision low-temperature fluid bath, gas boosters and specialty pumps, numerous gages and data-measurement or acquisition instruments, pressure vessels, and high-quality materials needed for our experiments. Our funding sources included: NASA (Planetary Geology and Geophysics Program), the USGS Gas Hydrates Project, the USGS Earthquake Science Center, Lawrence Livermore National Laboratory LDRD (Lab Directed Research & Development), direct DOE Awards, and DOE-sponsored interagency agreements with the USGS in support of the USGS Gas Hydrates Project.

## Special Acknowledgments

We wish to thank all our U.S. Geological Survey (USGS) Earthquake Science Center Directors, in particular: Mary Lou Zoback and Steve Hickman, who encouraged us over the years to write proposals to the National Aeronautics and Space Administration (NASA), Department of Energy, and Lawrence Livermore National Laboratory (LNL) to fund the research summarized in this report and provided floor space and machine shop facilities that made all of this work possible.

We also thank past and current Project Leaders of the USGS Gas Hydrate Project—Bill Dillon, Deborah Hutchinson, Carolyn Ruppel, and Tim Collett—for much of the laboratory support after the year 2000, and their invaluable help and advice over the years when our laboratory was active. They also provided access to numerous—and priceless—samples of natural gas hydrates recovered from field expeditions—samples that we otherwise would not have had the opportunity to image by cryo-SEM. Being the first to peer inside some of those samples was always exciting.

Bill Durham (LNL and later MIT) was our enthusiastic research partner from the beginning of our NASA supported research on the strength and rheologies of planetary ices, starting in 1978 and continuing to present day. This enthusiasm continued in the transition to clathrate hydrate research, work that included careful measurements of clathrate strength as well as our technically demanding collaboration with MBARI involving seafloor experiments described in this report. Bill also helped with the design of various equipment that we built in our laboratory, presented some of our work at scientific meetings, and coauthored more than a quarter of our publications.

We must acknowledge our pioneering and visionary USGS Menlo Park colleague, Keith Kvenvolden, for establishing the importance of hydrocarbon clathrate hydrates on planet Earth and their potential as non-traditional energy sources. Keith also led the way in establishing the first clathrate hydrate laboratory at the USGS Menlo Park facility and helped us navigate the world of clathrate hydrate research from early on. He also was welcoming of our material-science approach to clathrate hydrate research. Keith's ability to "cut to the chase" with his special humor was also valuable to us. The large and colorful map that he and Tom Lorenson created, showing the world-wide distribution of clathrate hydrates, graced the wall of our hydrate laboratory for many years as an inspiration.

From the beginning of our laboratory, we also benefitted enormously from the encouragement, vast knowledge, and expertise provided by Dendy Sloan and his group at Colorado School of Mines, which later also included its current leader (as of time of writing), Carolyn Koh. They were vocal advocates of our work, and several editions of their classic

textbook “Clathrate Hydrates of Natural Gases” remain on our bookshelves. Providing the formal book review for the second edition of this textbook in 2000 was an honor for Laura—not to mention an in-depth learning experience.

During the final 12 years of our laboratory, 2010 through 2022, Laura greatly enjoyed the highly productive collaboration with researchers from SIO and LLNL in obtaining first-ever electrical conductivity measurements on pure, end-member gas hydrates and related samples, initiated by Steve Constable (SIO), who also devoted considerable time into bringing DOE support for our work. His early concept to dovetail a laboratory-based experimental program (at USGS Menlo Park) with his field-based controlled-source electromagnetic work in the Gulf of Mexico and offshore California, resulted in a prolific series of coauthored publications that were a pleasure to work on.

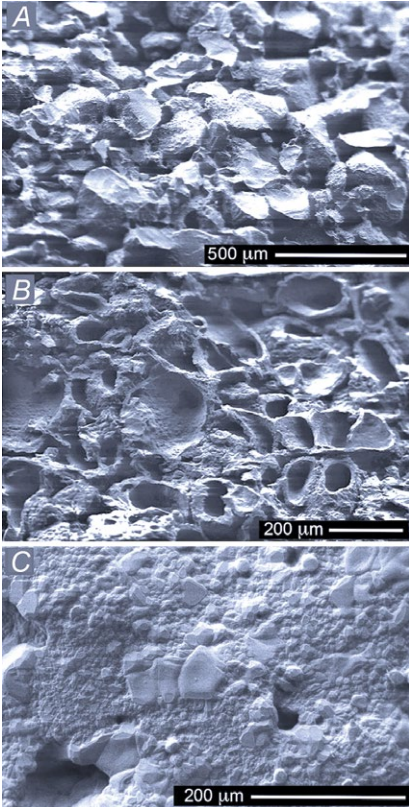
We are also deeply indebted to John Pinkston, our superb lab manager and chief lab engineer who, although infrequently listed as a coauthor, was involved in almost every phase of this research and was a key factor in the success of our laboratory. John’s persevering and good-natured personality greeted every technical challenge that we put before him. Although not trained as a laboratory engineer, he taught himself to be a skilled one.

We were blessed with the technical skills and design abilities of our USGS machinists and instrument-makers, the late Ben Hankins, and Dennis Mello, now retired. We are also grateful for the expertise and considerable assistance provided by Robert Oscarson, Leslie Hayden, and Dawn Ruth in the USGS Scanning Electron Microscopy Laboratory.

Lastly, we thank Bill Waite and Tom Lorenson (both USGS) for providing expert reviews of this Report, and Alex Lyles for his significant help with final editing.

## Appendix 1. Evolution of the Seed-Ice Reaction Model to Form Pure Methane Clathrate

Year, Paper (Appendix 2)	Observations and measurements	Interpretation of reaction model
1996, Paper 1 EARLY MODEL	<ul style="list-style-type: none"> <li>• Pressure-temperature-time (P-T-t) records of fully reacted methane (CH<sub>4</sub>) clathrate samples, using end-cap-emplaced thermocouples for thermal monitoring, showed some accumulation of melt during reaction but did not show P-T discontinuities associated with complete melting of the ice, despite full reaction requiring 8–12 hours above the H<sub>2</sub>O melting curve.</li> <li>• P-T-t histories of partially reacted samples taken to known extent of reaction, including mid-to-late stage, supported the above observations.</li> <li>• Conversely, companion tests using neon, a non-hydrate-forming gas, exhibited P-T-t histories fully consistent with complete melting of ice over a narrow thermal window upon crossing the ice point.</li> <li>• When optimal synthesis conditions were met, final clathrate sample textures were uniform from top to bottom with no pooled water at the base.</li> <li>• When optimal synthesis conditions were not met, melting textures were obvious as was the thermal signature for bulk melting.</li> </ul>	<ul style="list-style-type: none"> <li>• <u>Our initial model</u>: Clathrate forms “by a progressive reaction occurring at the nascent ice/liquid water interface. As reaction proceeds, the rate of melting of metastable H<sub>2</sub>O ice may be suppressed to allow short-lived superheating to at least 276 K.” (Paper 1)</li> <li>• After development of an outer clathrate shell, continued clathrate formation presumably involves solid-state diffusion of CH<sub>4</sub> gas to the ice core. We envisioned reaction as essentially a grain-for-grain conversion.</li> <li>• The hydrate surface layer not only rate-limits reaction in the ice grain interiors, but possibly “armors” the grain interiors from melting in bulk.</li> <li>• Might clathrate shells mask P reductions associated with ice melting from communicating with the gas P measurement system? We deemed this unlikely as it requires strong clathrate seals to form around ice grains during initial reaction when the clathrate layer is thin and presumably weak. The lack of an appreciable melting signature thus suggested temporary persistence of ice cores in a superheated state.</li> </ul>
1998, Papers 2–4	<ul style="list-style-type: none"> <li>• Optical cell experiments on both CH<sub>4</sub> and CO<sub>2</sub> hydrate showed initial, although minimal (≤ 2%), reaction occurring on ice grain surfaces at T well below the H<sub>2</sub>O liquidus upon first exposure to the hydrate former.</li> <li>• Upon further heating to T above the ice point, no collapse of the hydrate encasement was observed to suggest bulk melting of ice cores. Instead, grains maintained identifiable shapes and sizes.</li> <li>• In other tests, unreacted cores were induced to melt by greatly reducing the overpressure, resulting in rapid changes in grain shape and expulsion of water. The expelled water then quickly formed hydrate.</li> </ul>	<ul style="list-style-type: none"> <li>• Results from optical cell experiments supported our original shrinking-core model in which after thin shells of hydrate initially form on ice grain surfaces, subsequent formation occurs primarily by diffusion of gas through the hydrate shell and to the ice core.</li> <li>• The induced melting experiments indicated that by reducing the driving potential for continued clathrate reaction, bulk melting of unreacted cores proceeds quickly and is easily observable. The experiment also appeared to show that the core was still ice for over 0.5 hours at 3.5°C before induced to melt, further supporting superheated ice arguments.</li> </ul>
2000–2001, Papers 8 and 10	<ul style="list-style-type: none"> <li>• Relocating thermocouples to deep inside the sample chambers, in direct contact with reactants, revealed that significant melting of the seed ice does in fact take place. However, melting is neither complete nor rapid upon immediately crossing the ice point (0°C). Instead, it is spread out over a nearly 1-hour period during which central portions of samples remain near 0°C despite external bath T reaching 10°C.</li> <li>• Other emerging results from our lab revealed the exceptionally low thermal conductivity and high strength of CH<sub>4</sub> clathrate relative to ice, defying our own previous expectations.</li> </ul>	<ul style="list-style-type: none"> <li>• We partially revised our early model given new evidence for appreciable melting of ice, even though neither complete nor rapid melting was measured upon crossing the ice point.</li> <li>• Our improved understanding of the strength and thermal conductivity of CH<sub>4</sub> clathrate also shed insight on the “masking” properties of the hydrate shells.</li> <li>• Results by others (Moudrakovski et al., J. Phys. Chem. A., 1999, v. 103) demonstrated that hydrate-encased cores of melt could in fact maintain particle morphology, disproving our early supposition that thin rinds of hydrate could not act as seals that mask internal melting.</li> </ul>

Year, Paper ( )	Observations and measurements	Interpretation of reaction model
2004, Paper 42 FINAL MODEL	<ul style="list-style-type: none"> <li>• Cryo-SEM imaging of samples quenched mid-reaction revealed extensive recrystallization and changes to grain morphology and pore geometry, despite fabrication from rounded ice grains of known size.</li> <li>• Clathrate-encased grains develop into a tightly fitted arrangement with increased grain contact area upon progression of reaction. Some regions exhibit fractured, hollow, spheroidal shells of hydrate, coupled with evidence of core-melting.</li> <li>• Liquid from melting cores migrates to adjacent grain junctions, where it forms clathrate and further cements the sample. Pooling of melt is only observed when optimal synthesis conditions are not met.</li> <li>• Further recrystallization and annealing of grains accompanies the final hold at peak P-T conditions.</li> </ul>	<ul style="list-style-type: none"> <li>• <u>Our final, revised model</u>: Cryo-SEM imaging indicated that our original shrinking-core model did not accurately describe reaction of ice to clathrate at T above the ice point, despite formation rates appearing to support the model. Instead, the observed textural progression, combined with improved thermal modeling, shows: <ol style="list-style-type: none"> <li>1. Early but minimal clathrate growth occurs along ice grain surfaces at subsolidus conditions before the reactants are warmed above the ice melting curve. (<u>Panel A at left.</u>) Clathrate begins to form a thin shell encasing the ice core within.</li> <li>2. Above 0°C, reaction continues by the combined processes of diffusion of the clathrate-forming species through the developing clathrate shell to the ice core within, and progressive melting of the core that can lead to collapse of the shell and leakage of melt to adjacent regions. This melt is held in place by surface tension where it then forms clathrate. (<u>Panel B at left.</u>)</li> <li>3. Melting and reaction initiates in material in closest contact with sample-chamber walls and progresses inward due to heat flow gradients. This is evidenced by internal thermocouples monitoring the endothermic melting process, keeping local temperature buffered near 0°C. The center of samples can lag the external fluid bath T by nearly an hour, far longer than material in contact with the vessel base or walls.</li> <li>4. During late-stage reaction, the clathrate domains recrystallize, including the structure of the shells themselves. The reaction does not result in grain-for-grain conversion from the original seed ice grains; instead, final samples exhibit finely crystalline material with grainsize typically several tens of microns to upward of about 100 μm (<u>Panel C at left.</u>) Along cavity walls, clathrate crystals often display highly faceted and euhedral crystal growth (see Cover image.)</li> </ol> </li> <li>• <u>Other key conclusions</u>: The exceptionally high strength and low thermal conductivity of CH<sub>4</sub> clathrate can obscure the full P-T signature associated with the ice-to-water phase change during synthesis, a signature (or lack thereof) that formed the basis of our original superheated ice arguments.</li> <li>5. The very high strength presumably contributes to the sometimes-observed maintenance of grain shape integrity with little disruption of the outer shell, despite the volumetric changes associated with core-melting within.</li> <li>6. Insulating properties of the clathrate shell may serve to keep grain-core temperatures below those measured elsewhere in the sample chamber during the initial heating event.</li> </ul>
		
	<p><b>Methane clathrate formation by the seed-ice method.</b> (A) Early-stage growth of clathrate on ice grains, quenched upon reaching 0°C. (B) Mid-stage reaction shows thick clathrate shells surrounding empty cores from which melt migrated. (C) Fully reacted clathrate exhibits significant late-stage recrystallization after multiple hours at peak P-T conditions. Images from Papers 42 &amp; 56 in Appendix 2.</p>	

## Appendix 2. Annotated Publication List

Publications are listed in chronological order. Data release products, corrections, or other related information (such as cover photos) are listed as bullet points with relevant publications. Our 75 technical abstracts are not included in the list below.

1. Stern, L.A., Kirby, S.H., and Durham, W.B., 1996, Peculiarities of methane clathrate hydrate formation and solid-state deformation, including possible superheating of water ice: *Science*, v. 273, no. 5283, p. 1843–1848, <https://doi.org/10.1126/science.273.5283.1843>.
  - Cover photo *Science*: <https://science.sciencemag.org/content/sci/273/5283/local/front-matter.pdf>
  - Cover image *Science News*: <https://www.sciencenews.org/sn-magazine/november-9-1996>.
  - *Science News* feature on our postulation of superheated ice: [www.sciencenews.org/archive/materials-science-11](http://www.sciencenews.org/archive/materials-science-11) and inclusion of our work in “Science News of the Year”: [www.sciencenews.org/archive/science-news-year-13](http://www.sciencenews.org/archive/science-news-year-13) (Materials Science section).
2. Stern, L.A., Kirby, S.H., and Durham, W.B., 1997, Synthesis of polycrystalline methane hydrate, and its phase stability and mechanical properties at elevated pressure, in American Chemical Society, Division of Fuel Chemistry, 213th, San Francisco, Calif., April 13–17, 1997, Proceedings: American Chemical Society, Division of Fuel Chemistry, v. 42, no. 2, p. 544–550, <https://pubs.er.usgs.gov/publication/70019381>.
3. Stern, L.A., Kirby, S.H., and Durham, W.B., 1998a, Polycrystalline methane hydrate—Synthesis from superheated ice, and low-temperature mechanical properties: *Energy & Fuels*, v. 12, no. 2, p. 201–211, <https://doi.org/10.1021/ef970167m>.
  - American Chemical Society R.A. Glenn Award Paper, Fuel Division.
4. Stern, L.A., Hogenboom, D.L., Durham W.B., Kirby S.H., and Chou I-M., 1998b, Optical cell evidence for superheated ice under gas-hydrate-forming conditions: *Journal of Physical Chemistry B*, v. 102, no. 15, p. 2627–2632, <https://doi.org/10.1021/jp973108i>.
5. Circone, S., Stern, L.A., Kirby, S.H., Pinkston, J.C., and Durham, W.B., 2000, Pure methane hydrate dissociation rates at 0.1 MPa and temperatures above 272 K, in Holder, G.D., and Bishnoi, P.R., eds., *Gas hydrates—Challenges for the Future: Annals of the New York Academy of Sciences*, v. 912, no. 1, p. 544–556, <https://doi.org/10.1111/j.1749-6632.2000.tb06809.x>.
6. Dvorkin, J., Helgerud, M.B., Waite, W.F., Kirby, S.H., and Nur, A., 2000, Introduction to physical properties and elasticity models, chap. 20 in Max, M.D., ed., *Natural Gas Hydrate—In Oceanic and Permafrost Environments*: Springer, Dordrecht, v. 5, p. 245–261, [https://doi.org/10.1007/978-94-011-4387-5\\_20](https://doi.org/10.1007/978-94-011-4387-5_20).
7. Stern, L.A., 2000, Book review of Sloan, E.D., Jr., ed., *Clathrate Hydrates of Natural Gases* [2nd ed.], *Energy & Fuels*, v. 14, no. 5, p. 1123–1124, <https://doi.org/10.1021/ef000056e>
  - Invited contribution.
8. Stern, L.A., Kirby, S.H., Durham, W.B., Circone, S., and Waite, W.F., 2000, Laboratory synthesis of pure methane hydrate suitable for measurement of physical properties and decomposition behavior, chap. 25 in Max, M.D., ed., *Natural Gas Hydrate—In Oceanic and Permafrost Environments*: Springer, Dordrecht, p. 323–349, [https://link.springer.com/chapter/10.1007/978-94-011-4387-5\\_25](https://link.springer.com/chapter/10.1007/978-94-011-4387-5_25)
  - Invited contribution, including book cover photograph.
9. Waite, W.F., Helgerud, M.B., Nur, A., Pinkston, J.C., Stern, L.A., Kirby, S.H., and Durham, W.B., 2000, Laboratory measurements of compressional and shear wave speeds through pure methane hydrate, in Holder, G.D., and Bishnoi, P.R., eds., *Gas hydrates—Challenges for the Future: Annals of the New York Academy of Sciences*, v. 912, no. 1, p. 1003–1011, <https://doi.org/10.1111/j.1749-6632.2000.tb06855.x>.
10. Stern, L.A., Kirby, S.H., and Durham, W.B., 2001, Comment to the Moudrakovski et al. Letter, “Hydrate layers on ice particles and superheated ice—A <sup>1</sup>H NMR microimaging study”: *Journal of Physical Chemistry A*, v. 105, no. 7, p. 1223–1224, <https://doi.org/10.1021/jp994130+>.
11. Chou, I-M., Sharma, A., Burress, R.C., Shu, J., Mao, H-k., Hemley, R.J., Goncharov, A.F., Stern, L.A., and Kirby, S.H., 2001a, Transformations in methane hydrates: Proceedings of the National Academy of Sciences, v. 97, no. 25, p. 13484–13487, <https://doi.org/10.1073/pnas.250466497>.
12. Chou, I-M., Sharma, A., Burress, R.C., Hemley, R.J., Goncharov, A.F., Stern, L.A., and Kirby, S.H. 2001b, Diamond-anvil cell observations of a new methane hydrate phase in the 100-MPa pressure range: *Journal of Physical Chemistry A*, v. 105, no. 19, p. 4664–4668, <https://doi.org/10.1021/jp002735w>.



13. Circone, S., Kirby, S.H., Pinkston, J.P., and Stern, L.A., 2001, Measurement of gas yields and flow rates using a custom flow meter: Review of Scientific Instruments, v. 72, no. 6, p. 2709–2716, <https://doi.org/10.1063/1.1372173>.
14. deMartin, B.J., 2001, Laboratory measurements of the thermal conductivity and thermal diffusivity of methane hydrate at simulated in situ conditions: Atlanta, Ga., Georgia Institute of Technology, School of Earth and Atmospheric Sciences, M.S. thesis, 155 p., <https://smartech.gatech.edu/handle/1853/26216>.
- Experiments conducted in the Gas Hydrate Properties Laboratory under USGS supervision.
15. Helgerud, M.B., 2001, Wave speeds in gas hydrate and sediments containing gas hydrate—A laboratory and modeling study: Stanford, Calif., Stanford University, Ph.D. dissertation, 249 p., [https://earthsci.stanford.edu/research/srb/docs/theses/SRB\\_82\\_APR01\\_Helgerud.pdf](https://earthsci.stanford.edu/research/srb/docs/theses/SRB_82_APR01_Helgerud.pdf).
- Part of this thesis summarizes laboratory measurements in the Gas Hydrate Properties Laboratory in an apparatus designed and largely built by the USGS. Also, Kirby supervised this work and served on Helgerud’s Committee.
16. Stern, L.A., Circone, S., Kirby, S.H., and Durham, W.B. 2001a, Anomalous preservation of pure methane hydrate at 1 atm: Journal of Physical Chemistry B, v. 105, no. 9, p. 1756–1762, <https://doi.org/10.1021/jp003061s>.
17. Stern, L.A., Circone, S., Kirby, S.H., and Durham, W.B., 2001b, Preservation of methane hydrate at 1 atm: Energy & Fuels, v. 15, no. 2, p. 499–501, <https://doi.org/10.1021/ef000277k>.
18. Chakoumakos, B.C., Rawn, C.J., Rondinone, A.J., Marshall, S.L., Stern, L.A., Circone, S., Kirby, S.H., Jones, C.Y., Toby, B.H., and Ishii, Y., 2002, The use of rigid body constraints in Rietveld refinements of neutron diffraction data of clathrate hydrates, *in* International Conference on Gas Hydrates, 4th, Yokohama, Japan, May 19–23, 2002, Proceedings: International Conference on Gas Hydrates, v. 1, p. 655–658.
19. Freifeld, B.M., Kneafsey, T.J., Tomutsa, L., Stern, L.A., and Kirby, S.H., 2002, Use of computed X-ray tomographic data for analyzing the thermodynamics of a dissociating porous sand/hydrate mixture, *in* International Conference on Gas Hydrates, 4th, Yokohama, Japan, May 19–23, 2002, Proceedings: International Conference on Gas Hydrates, v. 1, p. 750–755, <https://escholarship.org/uc/item/6kp665p2>.
20. Helgerud, M.B., Circone, S., Stern, L.A., Kirby, S.H., and Lorensen, T.D., 2002, Measured temperature and pressure dependence of compressional and shear wave speeds in compacted, polycrystalline sII methane-ethane hydrate, *in* International Conference on Gas Hydrates, 4th, Yokohama, Japan, May 19–23, 2002, Proceedings: International Conference on Gas Hydrates, v. 1, p. 716–721.
21. Rawn, C.J., Rondinone, A.J., Chakoumakos, B.C., Marshall, S.L., Stern, L.A., Kirby, S.H., Jones, C.Y., Toby, B.H., and Ishii, Y., 2002, Neutron powder diffraction studies as a function of temperature of structure II hydrate formed from a methane + ethane gas mixture, *in* International Conference on Gas Hydrates, 4th, Yokohama, Japan, May 19–23, 2002, Proceedings: International Conference on Gas Hydrates, v. 1, p. 595–598.
22. Solem, R.C., Kastner, M., Stern, L.A., Kirby, S.H., Vollmer, M., and Paytan, A., 2002, Synthesis of a CH<sub>4</sub>-CFC hydrate, and an exchange experiment between a CH<sub>4</sub>-CFC gas and pure methane hydrate, *in* International Conference on Gas Hydrates, 4th, Yokohama, Japan, May 19–23, 2002, Proceedings: International Conference on Gas Hydrates, v. 1, p. 565–570.
23. Stern, L.A., Circone, S., Kirby, S.H., and Durham, W.B. 2002a, Reply to “Comments on Anomalous Preservation of pure methane hydrate at 1 atm”: Journal of Physical Chemistry B, v. 106, no. 1, p. 228–230, <https://doi.org/10.1021/jp012189m>.
24. Stern, L.A., Circone, S., Kirby, S.H., and Durham, W.B., 2002b, New insights into the phenomenon of anomalous or “self” preservation of gas hydrates, *in* International Conference on Gas Hydrates, 4th, Yokohama, Japan, May 19–23, 2002, Proceedings: International Conference on Gas Hydrates, v. 1, p. 673–677.
25. Stern, L.A., Kirby, S.H., and Circone, S. 2002c, Interagency group “zooms in” on methane hydrate pore structures: Fire in the Ice—The National Energy Technology Laboratory Methane Hydrate Newsletter, v. 2, no. 2, 8 p., <https://netl.doe.gov/sites/default/files/publication/HMNewsSummer02.pdf>.
26. Tomutsa, L., Freifeld, B., Kneafsey, T., and Stern, L.A., 2002, X-ray computed tomography observation of methane-hydrate dissociation *in* SPE Gas Technology Symposium, Calgary, Alberta, April 30–May 2, 2002, Proceedings: Society of Petroleum Engineers Gas Technology Symposium, paper SPE 75533, <https://doi.org/10.2118/75533-MS>.

27. Waite, W., Pinkston, J., and Kirby, S., 2002a, Preliminary laboratory thermal conductivity measurements in pure methane hydrate and methane hydrate-sediment mixtures, *in* International Conference on Gas Hydrates, 4th, Yokohama, Japan, May 19–23, 2002, Proceedings: International Conference on Gas Hydrates, v. 1, p. 728–733.
28. Waite, W.F., deMartin, B.J., Kirby, S.H., Pinkston, J., and Ruppel, C.D., 2002b, Thermal conductivity measurements in porous mixtures of methane hydrate and quartz sand: *Geophysical Research Letters*, v. 29, no. 24, 4 p., <https://doi.org/10.1029/2002GL015988>.
29. Chakoumakos, B.C., Rawn, C.J., Rondinone, A.J., Stern, L.A., Circone, S., Kirby, S.H., Ishii, Y., Jones, C.Y., and Toby, B.H., 2003, Temperature dependence of polyhedral cage volumes in clathrate hydrates: *Canadian Journal of Physics*, v. 81, nos. 1–2, p. 183–189, <https://doi.org/10.1139/p02-141>.
30. Circone, S., Stern, L.A., Kirby, S.H., Durham, W.B., Chakoumakos, B.C., Rawn, C.J., Rondinone, A.J., and Ishii, Y., 2003, CO<sub>2</sub> hydrate—Synthesis, composition, dissociation behavior, and a comparison to structure I CH<sub>4</sub> hydrate: *Journal of Physical Chemistry B*, v. 107, no. 23, p. 5529–5539, <https://doi.org/10.1021/jp027391j>.
31. Durham, W.B., Kirby, S.H., Stern, L.A., and Zhang, W., 2003a, The strength and rheology of methane clathrate hydrate: *Journal of Geophysical Research*, v. 108, no. B4, p. 2182–2193, <https://doi.org/10.1029/2002JB001872>.
- Correction to “The strength and rheology of methane clathrate hydrate”: *Journal of Geophysical Research*, v. 108, no. B6, <https://doi.org/10.1029/2003JB002534>.
32. Durham, W.B., Stern, L.A., and Kirby, S.H., 2003b, Ductile flow of methane hydrate: *Canadian Journal of Physics*, v. 81, nos. 1–2, p. 373–380, <https://doi.org/10.1139/p03-042>.
33. Helgerud, M.B., Waite, W.F., Kirby, S.H., and Nur, A., 2003a, Measured temperature and pressure dependence of  $V_p$  and  $V_s$  in compacted, polycrystalline sI methane and sII methane-ethane hydrate: *Canadian Journal of Physics*, v. 81, nos. 1–2, p. 47–53, <https://doi.org/10.1139/p03-016>.
34. Helgerud, M.B., Waite, W.F., Kirby, S.H., and Nur, A., 2003b, Measured temperature and pressure dependence of compressional ( $V_p$ ) and shear ( $V_s$ ) wave speeds in compacted, polycrystalline ice Ih: *Canadian Journal of Physics*, v. 81, nos. 1–2, p. 81–87, <https://doi.org/10.1139/p03-008>.
35. Rawn, C.J., Rondinone, A.J., Chakoumakos, B.C., Circone, S., Stern, L.A., Kirby, S.H., and Ishii, Y., 2003, Neutron powder diffraction studies as a function of temperature of structure II hydrate formed from propane: *Canadian Journal of Physics*, v. 81, nos. 1–2, p. 431–438, <https://doi.org/10.1139/p03-022>.
36. Stern, L.A., Circone, S., Kirby, S.H., and Durham, W.B., 2003, Temperature, pressure, and compositional effects on anomalous or “self” preservation of gas hydrates: *Canadian Journal of Physics*, v. 81, nos. 1–2, p. 271–283, <https://doi.org/10.1139/p03-018>.
37. Circone, S., Stern, L.A., and Kirby, S.H., 2004a, The role of water in gas hydrate dissociation: *Journal of Physical Chemistry B*, v. 108, no. 18, p. 5747–5755, <https://doi.org/10.1021/jp0362584>.
38. Circone, S., Stern, L.A., and Kirby, S.H., 2004b, The effect of elevated methane pressure on methane hydrate dissociation: *American Mineralogist*, v. 89, nos. 8–9, p. 1192–1201, <https://doi.org/10.2138/am-2004-8-905>.
39. Kirby, S.H., Stern, L.A., Circone, S., and Pinkston, J., 2004a, Hydrate decomposition under scrutiny: Fire in the Ice—The National Energy Technology Laboratory Methane Hydrate Newsletter, v. 4, no. 1, 6 p., <https://www.netl.doe.gov/sites/default/files/publication/HMNewsWinter04.pdf>.
40. Kirby, S.H., Circone, S., Stern, L.A., and Pinkston, J., 2004b, USGS laboratory studies shed light on hydrate decomposition behavior under possible gas production scenarios: Fire in the Ice—The National Energy Technology Laboratory Methane Hydrate Newsletter, v. 4, no. 3, p. 5–9, <https://netl.doe.gov/sites/default/files/publication/HMNewsSummer04.pdf>.
41. Rehder, G., Kirby, S.H., Durham, W.B., Stern, L.A., Peltzer, E.T., Pinkston, J., and Brewer, P.G., 2004, Dissolution rates of pure methane hydrate and carbon-dioxide hydrate in undersaturated seawater at 1000-m depth: *Geochimica et Cosmochimica Acta*, v. 68, no. 2, p. 285–292, <https://doi.org/10.1016/j.gca.2003.07.001>.
42. Stern, L.A., Kirby, S.H., Circone, S., and Durham, W.B., 2004, Scanning Electron Microscopy investigations of laboratory-grown gas hydrates formed from melting ice, and comparison to natural hydrates: *American Mineralogist*, v. 89, nos. 8–9, p. 1162–1175, <https://doi.org/10.2138/am-2004-8-902>.
43. Circone, S., Kirby, S.H., and Stern, L.A., 2005a, Direct measurement of methane hydrate composition along the hydrate equilibrium boundary: *Journal of Physical Chemistry B*, v. 109, no. 19, p. 9468–9475, <https://doi.org/10.1021/jp0504874>.
44. Circone, S., Stern, L.A., and Kirby, S.H., 2005b, Thermal regulation of methane hydrate dissociation—Implications for gas production models: *Energy & Fuels*, v. 19, no. 6, p. 2357–2363, <https://doi.org/10.1021/ef0500437>.
45. Durham, W.B., Stern, L.A., Kirby, S.H., and Circone, S., 2005, Rheological comparisons and structural imaging of sI and sII end-member gas hydrates and hydrate/sediment aggregates, *in* International Conference on Gas Hydrates, 5th, Trondheim, Norway, June 13–16, 2005, Proceedings: International

- Conference on Gas Hydrates, v. 2, p. 607–614, paper 2030, <https://web.mit.edu/wbdurham/www1/papers/83-Durham-rheol-ICGH%2705.pdf>
46. Hoshikawa, A., Igawa, N., Uemauchi, H., Ishii, Y., and Stern, L.A., 2005, Maximum entropy method analysis of neutron powder diffraction patterns of methane deuterohydrates, *in* International Conference on Gas Hydrates, 5th, Trondheim, Norway, June 13–16, 2005, Proceedings: International Conference on Gas Hydrates, v. 5, p. 1619–1626 paper 5028, <https://www.proceedings.com/05337.html>.
47. Stern, L.A., and Kirby, S.H., 2005, Grain and pore structure imaging of gas hydrate from core MD02-2569 (Mississippi Canyon, Gulf of Mexico)—A first look by scanning electron microscope (SEM), chap. 12 *in* Winters, W.J., Lorenson, T.D., and Paull, C.K., eds., Initial report on gas hydrate and paleo-climate results from the RSV Marion-Dufresne Cruise in the Gulf of Mexico, July 2–18, 2003: U.S. Geological Survey Open-File Report 2004–1358, 8 p., [https://cmgds.marine.usgs.gov/publications/of2004-1358/pdf\\_chapters/Chapter12.pdf](https://cmgds.marine.usgs.gov/publications/of2004-1358/pdf_chapters/Chapter12.pdf).
48. Stern, L.A., Kirby, S.H., and Durham, W.B., 2005a, Scanning electron microscope imaging of grain structure and phase distribution within gas-hydrate-bearing intervals from JAPEX/JNOC/GSC et al. Mallik well 5L-38—What can we learn from comparisons with laboratory-synthesized samples?: Geological Survey of Canada Bulletin 585, paper 31, <https://doi.org/10.4095/220811>.
49. Stern, L.A., Circone, S., Kirby, S.H., and Durham, W.B., 2005b, SEM imaging of gas hydrate formation processes and growth textures, and comparison to natural hydrates of marine and permafrost origin, *in* International Conference on Gas Hydrates, 5th, Trondheim, Norway, June 13–16, 2005, Proceedings: International Conference on Gas Hydrates, v. 1, p. 300–309, paper 1046, <https://www.proceedings.com/05337.html>.
50. Tait, K., Zhao, Y., Downs, R., Stern, L., and Kirby, S., 2005, Investigations into the stability, morphology, and the crystal structure of structure I and structure II methane-ethane clathrate hydrates, *in* International Conference on Gas Hydrates, 5th, Trondheim, Norway, June 13–16, 2005, Proceedings: International Conference on Gas Hydrates, v. 2, p. 541–544, paper 2021, <https://www.proceedings.com/05337.html>.
51. Circone, S., Kirby, S.H., and Stern, L.A., 2006, Thermodynamic calculations in the system CH<sub>4</sub>-H<sub>2</sub>O and methane hydrate phase equilibria: Journal of Physical Chemistry B, v. 110, p. 8232–8239, <https://doi.org/10.1021/jp055422f>.
52. Waite, W.F., Stern, L.A., Kirby, S.H., Winters, W.J., and Mason, D.H., 2007, Simultaneous determination of thermal conductivity, thermal diffusivity and specific heat in sI methane hydrate: Geophysical Journal International, v. 169, no. 2, p. 767–774, <https://doi.org/10.1111/j.1365-246X.2007.03382.x>.
53. Stern, L.A., and Kirby, S.H., 2008, Natural gas hydrates up close—A comparison of grain characteristics of samples from marine and permafrost environments as revealed by cryogenic SEM, *in* International Conference on Gas Hydrates, 6th, Vancouver, British Columbia, July 6–10, 2008, Proceedings: International Conference on Gas Hydrates, 12 p., paper 5330, <https://open.lib.ubc.ca/media/stream/pdf/59278/1.0041020/3>.
54. Helgerud, M.B., Waite, W.F., Kirby, S.H., and Nur, A., 2009, Elastic wave speeds and moduli in polycrystalline ice Ih, sI methane hydrate, and sII methane-ethane hydrate: Journal of Geophysical Research, v. 114, no. B2, <https://doi.org/10.1029/2008JB006132>.
- Correction to “Elastic wave speeds and moduli in polycrystalline ice Ih, sI methane hydrate, and sII methane-ethane hydrate”: Journal of Geophysical Research, v. 114, no. B4, <https://doi.org/10.1029/2009JB006451>.
55. Chen, P.-C., Huang, W.-L., and Stern, L.A., 2010, Methane hydrate synthesis from ice—Influence of pressurization and additives on optimizing formation rates and hydrate yield: Energy & Fuels, v. 24, no. 4, p. 2390–2403, <https://doi.org/10.1021/ef901403r>.
56. Du Frane, W.L., Stern, L.A., Weitemeyer, K.A., Constable, S., Pinkston, J.C., and Roberts, J.J., 2011a, Electrical conductivity of laboratory-synthesized methane hydrate, *in* International Conference on Gas Hydrates, 7th, Edinburgh, United Kingdom, July 17–21, 2011, Proceedings: International Conference on Gas Hydrates, 10 p., <https://www.osti.gov/servlets/purl/1183530/>.
57. Du Frane, W.L., Stern, L.A., Weitemeyer, K.A., Constable, S., Pinkston, J.C., and Roberts, J.J., 2011b, Electrical properties of polycrystalline methane hydrate: Geophysical Research Letters, v. 38, no. 9, 5 p., <https://doi.org/10.1029/2011GL047243>.
58. Du Frane, W.L., Stern, L.A., Weitemeyer, K.A., Constable, S., and Roberts, J. 2011c, Electrical resistivity of methane hydrate + sediment mixtures: Fire in the Ice—The National Energy Technology Laboratory Methane Hydrate Newsletter, v. 11, no. 2, 4 p., <https://netl.doe.gov/sites/default/files/publication/MHNews-2011-12.pdf>.

59. Hunt, A.G., Pohlman, J.W., Stern, L.A., Ruppel, C., Moscati, R.J., Landis, G.P., and Pinkston, J., 2011, Observations of mass fractionation of noble gases in synthetic methane hydrate, *in* International Conference on Gas Hydrates, 7th, Edinburgh, United Kingdom, July 17–21, 2011, Proceedings: International Conference on Gas Hydrates, 6 p. [https://www.researchgate.net/publication/259863200\\_Observations\\_of\\_mass\\_fractionation\\_of\\_noble\\_gases\\_in\\_synthetic\\_methane\\_hydrate/link/02e7e52e7baa9cd17e000000/download](https://www.researchgate.net/publication/259863200_Observations_of_mass_fractionation_of_noble_gases_in_synthetic_methane_hydrate/link/02e7e52e7baa9cd17e000000/download).
60. Stern, L.A., Lorenson, T.D., and Pinkston, J.C., 2011, Gas hydrate characterization and grain-scale imaging of recovered cores from the Mount Elbert gas hydrate stratigraphic test well, Alaska North Slope: *Marine and Petroleum Geology*, v. 28, no. 2, p. 394–403, <https://doi.org/10.1016/j.marpetgeo.2009.08.003>.
61. Hunt, A.G., Stern, L., Pohlman, J.W., Ruppel, C., Moscati, R.J., and Landis, G.P., 2013a, Mass fractionation of noble gases in synthetic methane hydrate—Implications for naturally occurring methane gas hydrate dissociation: *Chemical Geology*, v. 339, no. 1, p. 242–250, <https://doi.org/10.1016/j.chemgeo.2012.09.033>.
62. Hunt, A., Ruppel, C., Stern, L., and Pohlman, J., 2013b, Using noble gas signatures to fingerprint gas streams derived from dissociating methane hydrate: *Fire in the Ice—The National Energy Technology Laboratory Methane Hydrate Newsletter*, v. 13, no. 2, p. 23–26, [https://www.netl.doe.gov/sites/default/files/publication/MHNNews\\_2013\\_October.pdf](https://www.netl.doe.gov/sites/default/files/publication/MHNNews_2013_October.pdf).
63. Brewer, P.G., Peltzer, E.T., Walz, P.M., Kirby, S.H., Stern, L.A., and Pinkston, J.P., 2014a, Deep sea field test of the CH<sub>4</sub> hydrate to CO<sub>2</sub> hydrate spontaneous conversion hypothesis, *in* International Conference on Gas Hydrates, 8th, Beijing, China, July 28–August 1, 2014, Proceedings: International Conference on Gas Hydrates, paper T4-23, 9 p.
64. Brewer, P.G., Peltzer, E.T., Walz, P.M., Coward, E.K., Stern, L.A., Kirby, S.H., and Pinkston, J.P., 2014b, Deep sea field test of the CH<sub>4</sub> hydrate to CO<sub>2</sub> hydrate spontaneous conversion hypothesis: *Energy & Fuels*, v. 28, no. 11, p. 7061–7069, <https://dx.doi.org/10.1021/ef501430h>.
65. Stern, L.A., and Lorenson, T.D., 2014, Grain-scale imaging and compositional characterization of cryo-preserved India NGHP 01 gas-hydrate-bearing cores: *Marine and Petroleum Geology*, v. 58, part A, p. 206–222, <https://dx.doi.org/10.1016/j.marpetgeo.2014.07.027>.
66. Winters, W.J., Wilcox-Cline, R.W., Long, P., Dewri, S.K., Kumar, P., Stern, L., and Kerr, L., 2014, Comparison of physical and geotechnical properties of sediment from offshore India and other hydrate reservoirs: *Marine and Petroleum Geology*, v. 58, part A, p. 139–167, <https://dx.doi.org/10.1016/j.marpetgeo.2014.07.024>.
67. Du Frane, W.L., Stern, L.A., Weitemeyer, K.A., Constable, S., Smith, M.M., and Roberts, J.J., 2015, Electrical properties of methane hydrate plus sediment mixtures: *Journal of Geophysical Research*, v. 120, no. 7, p. 4773–4783, <https://dx.doi.org/10.1002/2015JB011940>.
68. Jang, J., Cao, S., Stern, L., Jung, J., and Waite, W., 2018, Impact of pore fluid chemistry on fine-grained sediment fabric and compressibility: *Journal of Geophysical Research*, v. 123, no. 7, p. 5495–5514, <https://doi.org/10.1029/2018JB015872>.
  - Jang, J., Cao, S.C., Stern, L.A., Waite, W.F. and Jung, J., 2018a, Effect of pore fluid chemistry on the sedimentation and compression behavior of pure, endmember fines: U.S. Geological Survey data release, <https://doi.org/10.5066/F77M076K>.
69. Lu, R., Stern, L.A., Du Frane, W.L., Pinkston, J.C., and Constable, S., 2018, Electrical conductivity of methane hydrate with pore fluids—New results from the lab: *Fire in the Ice—Methane Hydrate News*, v. 18, no. 1, p. 7–11, [https://netl.doe.gov/sites/default/files/publication/MHNNews\\_2018\\_Summer.pdf](https://netl.doe.gov/sites/default/files/publication/MHNNews_2018_Summer.pdf).
70. Jang, J., Waite, W.F., Stern, L.A., Collett, T.S., and Kumar, P., 2019a, Physical property characteristics of gas hydrate-bearing reservoir and associated seal sediments collected during NGHP-02 in the Krishna-Godavari Basin, in the offshore of India: *Journal of Marine and Petroleum Geology*, v. 108, no. 1, p. 249–271, <https://doi.org/10.1016/j.marpetgeo.2018.09.027>.
  - Jang, J., Waite, W.F., Stern, L.A., Collett T.S., and Kumar, P., 2019b, Dependence of sedimentation behavior on pore-fluid chemistry for sediment collected from Area B, Krishna-Godavari Basin, during India's National Gas Hydrate Program, NGHP-02: U.S. Geological Survey data release, <https://doi.org/10.5066/P9FXJ1VX>.
71. Jang, J., Dai, S., Yoneda, J., Waite, W.F., Stern, L.A., Boze, L-G., Collett, T., and Kumar, P., 2019c, Pressure core analysis of geomechanical and fluid flow properties of seals associated with gas hydrate-bearing reservoirs in the Krishna-Godavari Basin, offshore India: *Marine and Petroleum Geology*, v. 108, no. 1, p. 537–550, <https://doi.org/10.1016/j.marpetgeo.2018.08.015>.
72. Lu, R., Stern, L.A., Du Frane, W.L., Pinkston, J.C., Roberts, J.J., and Constable, R.S., 2019, The effect of brine on the electrical properties of methane hydrate: *Journal of Geophysical Research—Solid Earth*, v. 124, no. 11, p. 10877–10892, <https://doi.org/10.1029/2019JB018364>.

73. Constable, S., Lu, R., Kannberg, P., Stern, L., Du Frane, W., and Roberts, J. 2020a, In-situ and laboratory evidence for high electrical anisotropy in marine hydrate: Fire in the Ice—Methane Hydrate News, v. 20, no. 1, p. 1–4, [https://www.netl.doe.gov/sites/default/files/publication/MHNNews\\_Spring\\_2020.pdf](https://www.netl.doe.gov/sites/default/files/publication/MHNNews_Spring_2020.pdf).
74. Constable, S., Lu, R., Stern, L.A., Du Frane, W.L., and Roberts, J.J., 2020b, Laboratory electrical conductivity of marine gas hydrate: Geophysical Research Letters, v. 47, no. 16, 8 p., <https://doi.org/10.1029/2020GL087645>.
- Cover photograph for the volume also from GHPL: <https://agupubs.onlinelibrary.wiley.com/doi/epdf/10.1002/grl.59078>.
75. Jang, J., Waite, W., and Stern, L.A., 2020a, Gas hydrate petroleum systems—What constitutes the “seal”? Interpretation, v. 8, no. 2, p. T231–T248, <https://dx.doi.org/10.1190/INT-2019-0026.1>.
76. Jang, J., Cao, S.C., Stern, L.A., Waite, W.F., Jung, J., and Lee, J.Y., 2020b, Potential freshening impacts on fines migration and pore-throat clogging during gas hydrate production—2-D micromodel study with diatomaceous UBGH2 sediments: Marine and Petroleum Geology, v. 116, article 104244, 13 p., <https://doi.org/10.1016/j.marpetgeo.2020.104244>.
- Jang, J., Stern, L.A., Waite, W.F., Cao, S.C., Jung, J., and Lee, J.Y., 2020c, Dependence of sedimentation behavior on pore-fluid chemistry for sediment collected offshore South Korea during the Second Ulleung Basin Gas Hydrate Expedition, UBGH2: U.S. Geological Survey data release, <https://doi.org/10.5066/P9UJOYVR>.
77. Stern, L., Constable, S., Lu, R., Du Frane, W., and Roberts, J., 2021a, Electrical conductivity of CO<sub>2</sub> hydrate and CH<sub>4</sub> hydrate—Role of the guest molecule: Fire in the Ice—Methane Hydrate News, v. 21, no. 1, p. 9–12, [https://netl.doe.gov/sites/default/files/publication/MHNNews\\_Spring2021\\_0.pdf](https://netl.doe.gov/sites/default/files/publication/MHNNews_Spring2021_0.pdf).
78. Stern, L.A., Constable, S., Lu, R., Du Frane, W.L., and Roberts, J.J., 2021b, Electrical properties of carbon dioxide hydrate—Implications for monitoring CO<sub>2</sub> in the gas hydrate stability zone: Geophysical Research Letters, v. 48, no. 15, 9 p., <https://doi.org/10.1029/2021GL093475>.
79. Jang, J., Waite, W.F., Stern, L.A., and Yee, J.Y., 2022, Diatom influence on the production characteristics of hydrate-bearing sediments—Examples from Ulleung Basin, offshore South Korea: Marine and Petroleum Geology, v. 144, 19 p., <https://doi.org/10.1016/j.marpetgeo.2022.105834>.
- Jang, J., Waite, W.F., Stern, L.A., and Lee, J.Y., 2022a, Dataset of diatom controls on the compressibility and permeability of fine-grained sediment collected offshore of South Korea during the Second Ulleung Basin Gas Hydrate Expedition, UBGH2: U.S. Geological Survey data release, <https://doi.org/10.5066/P9ZLO4IM>.
  - Jang, J., Waite, W.F., Stern, L.A., and Lee, J.Y., 2022b, Dataset of diatom controls on the sedimentation behavior of fine-grained sediment collected offshore of South Korea during the Second Ulleung Basin Gas Hydrate Expedition, UBGH2: U.S. Geological Survey data release, <https://doi.org/10.5066/P9S6S24N>.
80. Constable, S., and Stern, L.A., 2022, Monitoring offshore CO<sub>2</sub> sequestration using marine CSEM methods; constraints inferred from field- and laboratory-based gas hydrate studies: Energies, v. 15, no. 19, p. 7411. (Special volume: “Gas Hydrate Energy Technologies for Net-Zero Carbon Emission”). <https://doi.org/10.3390/en15197411>.

## Other:

81. Wessells, S.M., ed., 2012, USGS Gas Hydrates Lab: U.S. Geological Survey video, <https://www.youtube.com/watch?v=U46XOoU0DrM>.

